Supplementary Information

π-Carbazolyl supported bis(alkyl) complexes of Sc, Y and La for α-olefin polymerization and hydrogenation

Alexander N. Selikhov[a,b] Polina V. Pechenkina,[b] Anton V. Cherkasov,[b] Yulia V. Nelyubina,[a] Tatyana A. Kovylina[b] and Alexander A. Trifonov,*[a,b]

[a.] *A. N. Nesmeyanov Institute of Organoelement Compounds of Russian Academy of Sciences, 28 Vavilova str., 119991, Moscow, GSP-1, Russia.*

[b.] *G. A. Razuvaev Institute of Organometallic Chemistry of Russian Academy of Sciences 603137, 49 Tropinina str., Nizhny Novgorod Russia GSP-445, Fax: + 007-831-462-74-97 E-mail: trif@iomc.ras.ru.*

Table of Contents

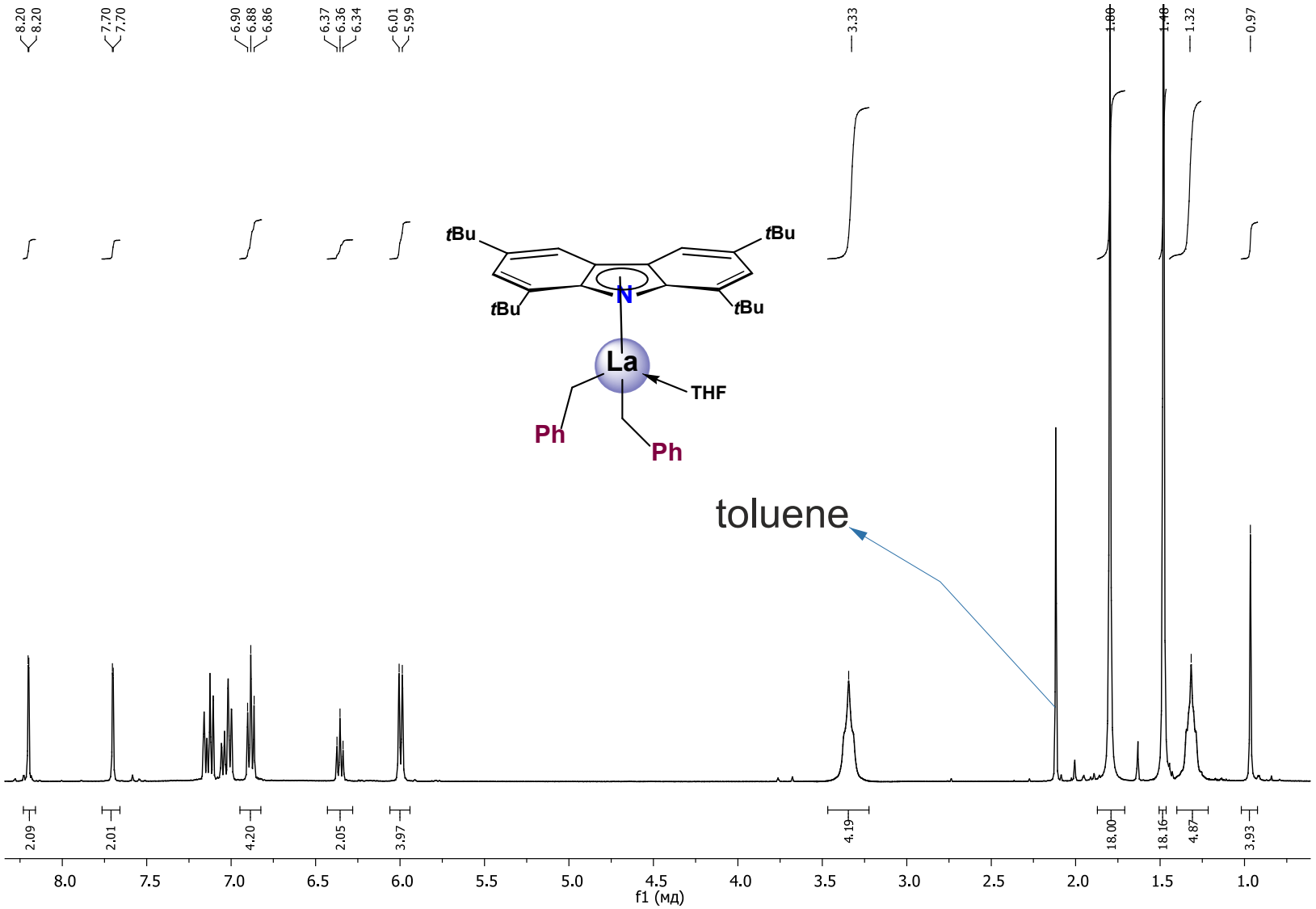

Figure S1. ^{1}H NMR spectrum of [*t*Bu$_4$Carb]La(CH$_2$C$_6$H$_5$)$_2$(THF) (**1-La**) (400 MHz, C$_6$D$_6$, 293 K).

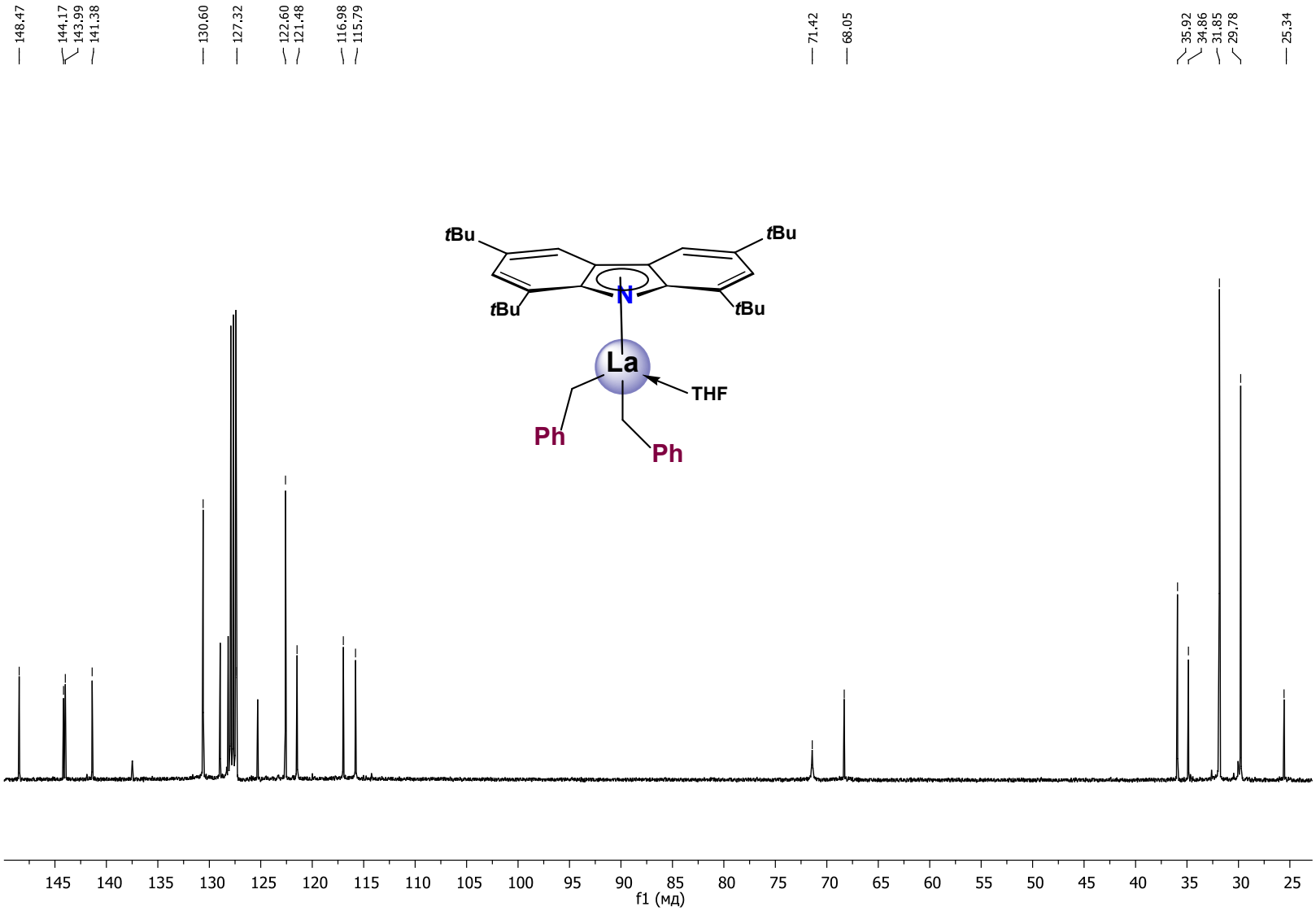

Figure S2. $^{13}C\{^{1}H\}$ NMR spectrum of [*t*Bu$_4$Carb]La(CH$_2$C$_6$H$_5$)$_2$(THF) (**1-La**) (100 MHz, C$_6$D$_6$, 293 K).

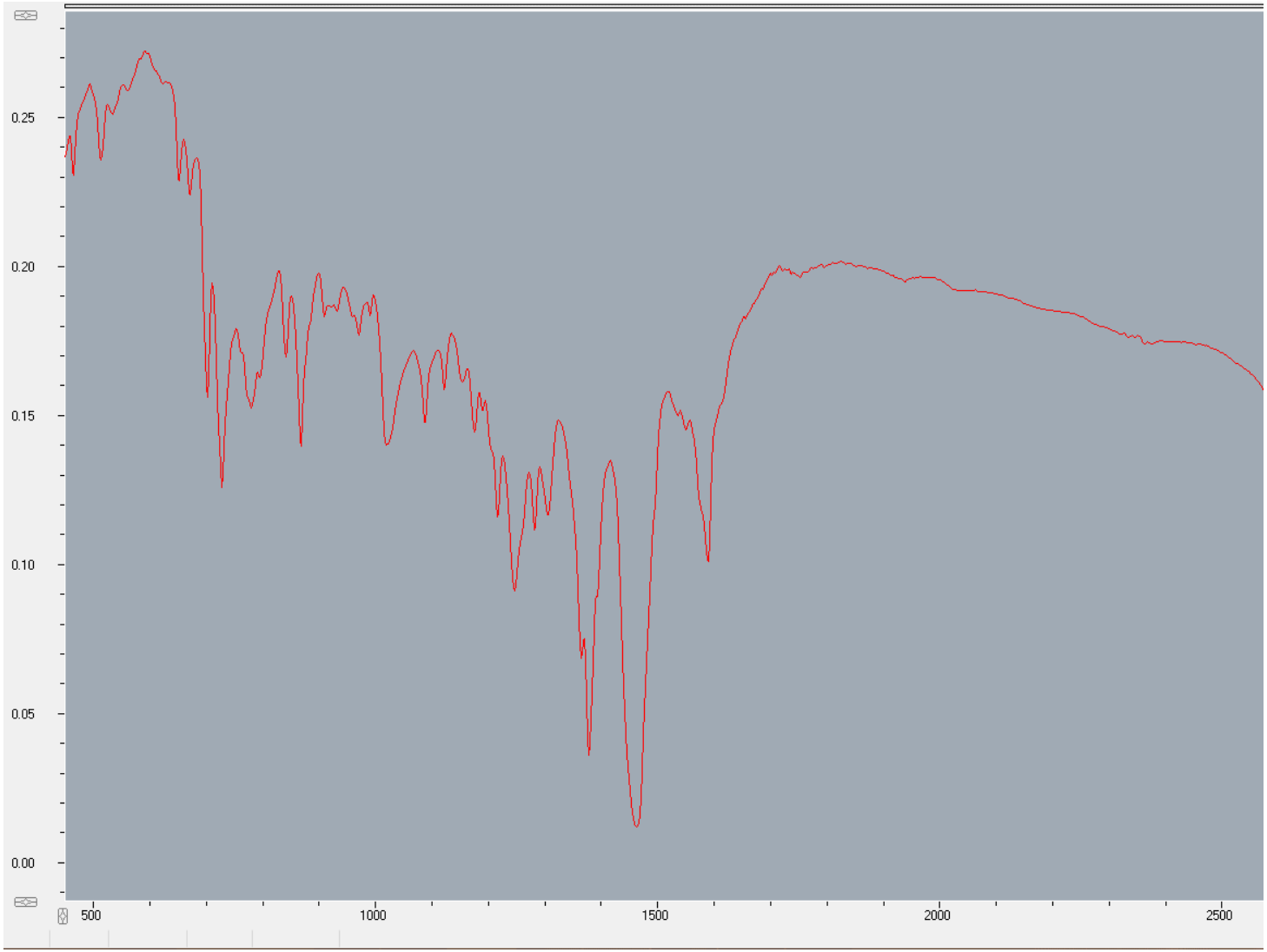

Figure S3. IR spectrum of complex [*t*Bu$_4$Carb]La(CH$_2$C$_6$H$_5$)$_2$(THF) (**1-La**) (KBr, Nujol mull).

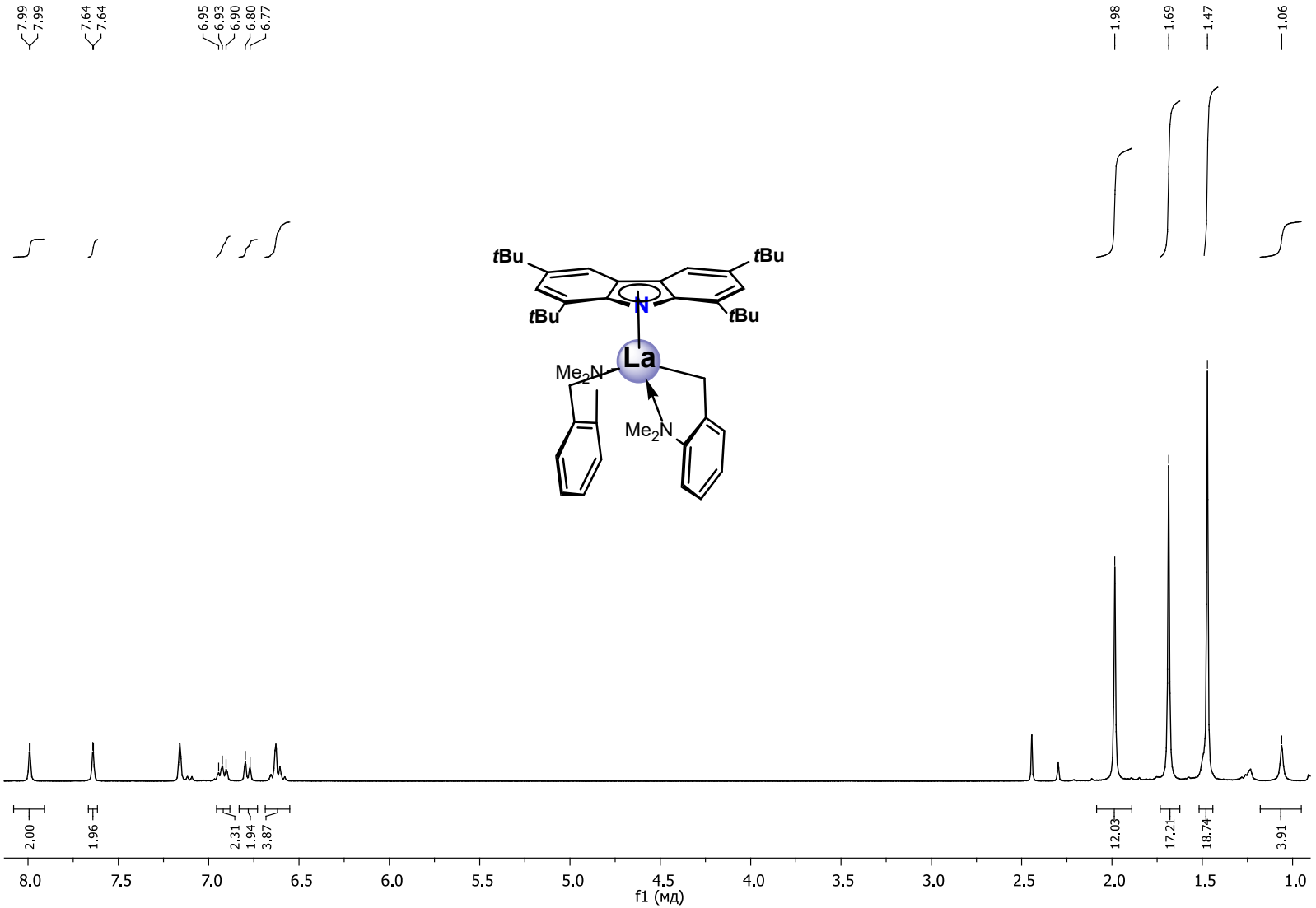

Figure S4. ^{1}H NMR spectrum of [*t*Bu$_4$Carb]La(*o*-NMe$_2$C$_6$H$_5$CH$_2$)$_2$ (**2-La**) (300 MHz, C$_6$D$_6$, 293 K).

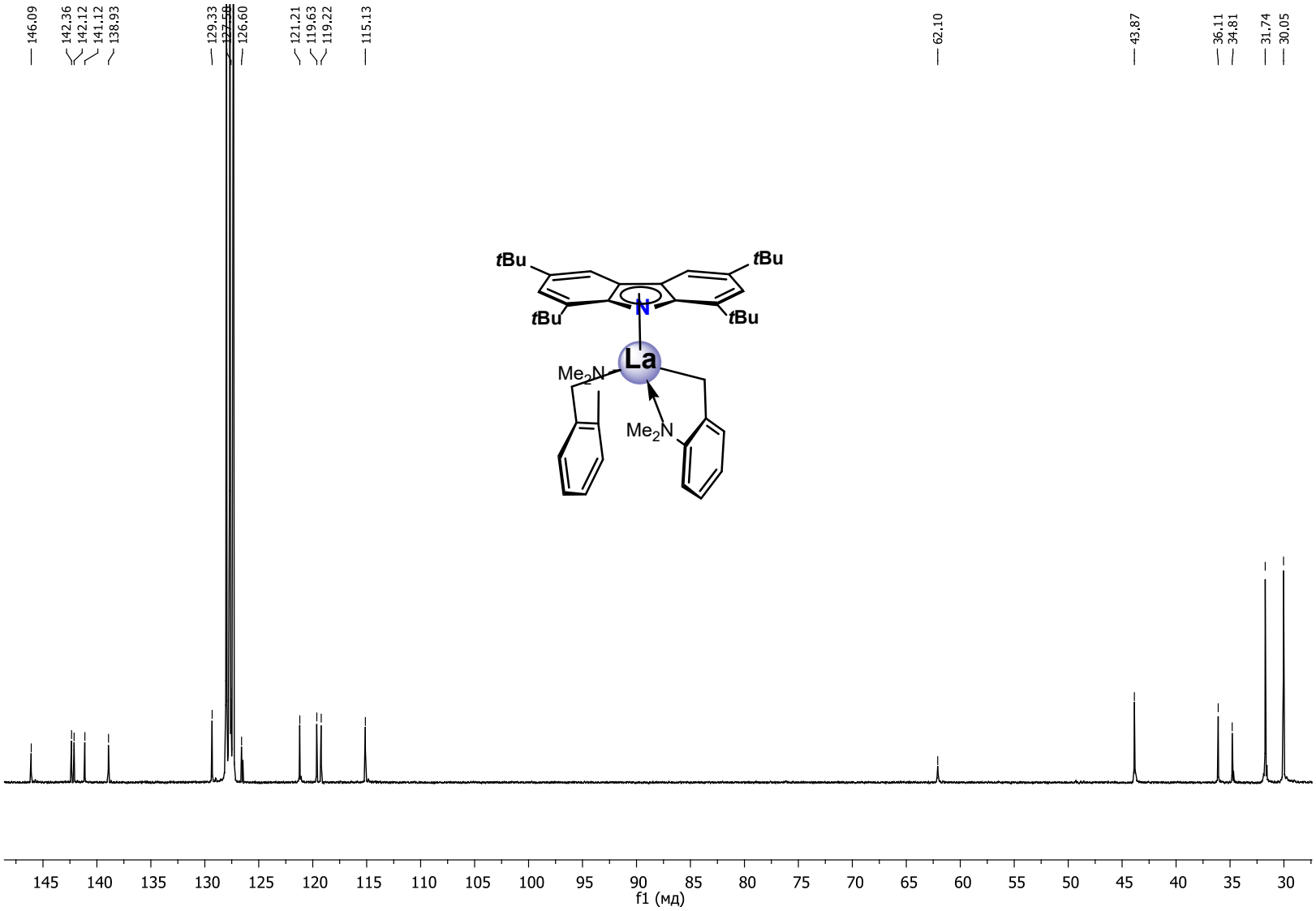

Figure S5. $^{13}C\{^{1}H\}$ NMR spectrum of [*t*Bu$_4$Carb]La(*o*-NMe$_2$C$_6$H$_5$CH$_2$)$_2$ (**2-La**) (75 MHz, C$_6$D$_6$, 293 K).

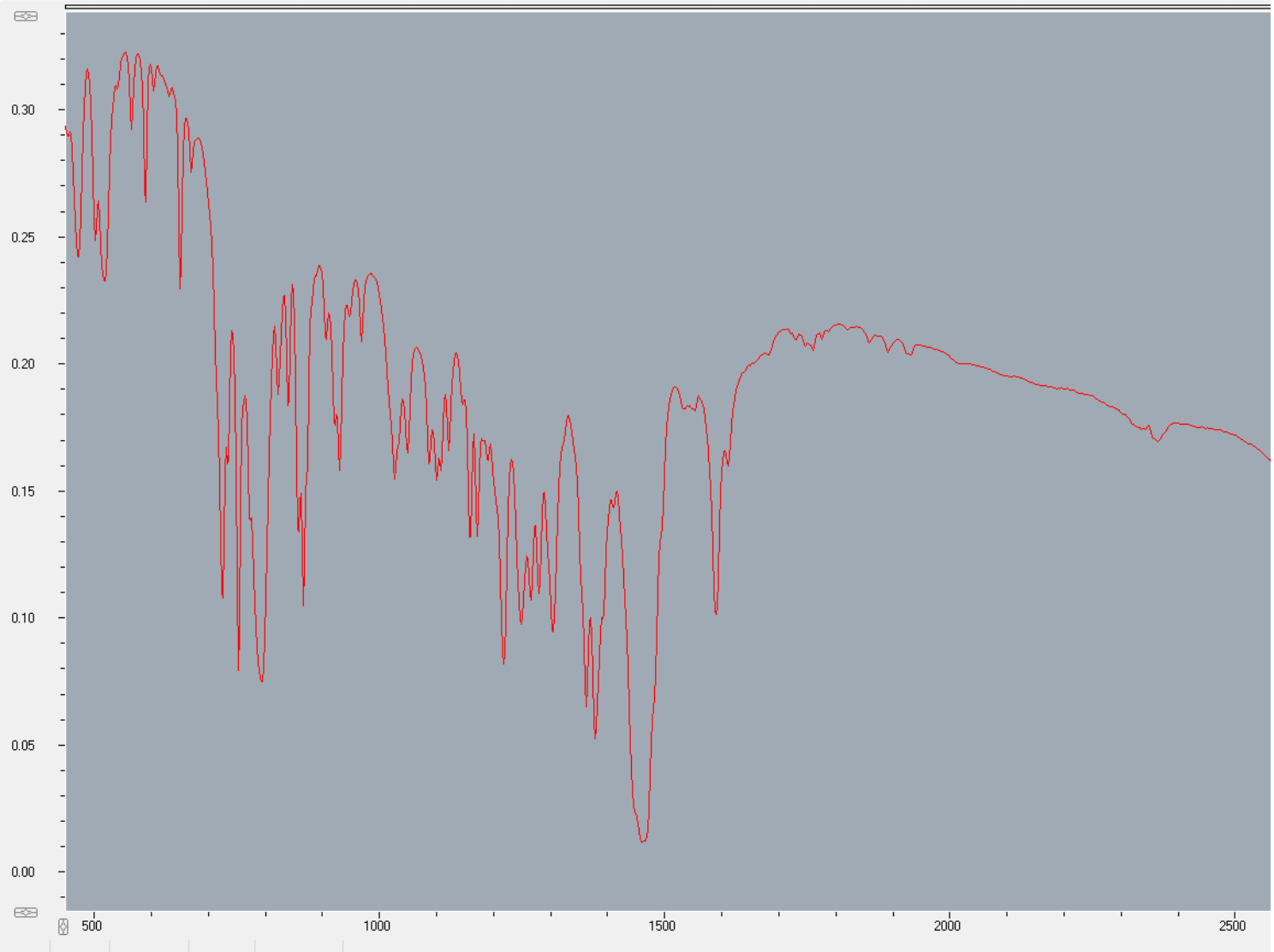

Figure S6. IR spectrum of complex [*t*Bu$_4$Carb]La(*o*-NMe$_2$C$_6$H$_5$CH$_2$)$_2$ (**2-La**) (KBr, Nujol mull).

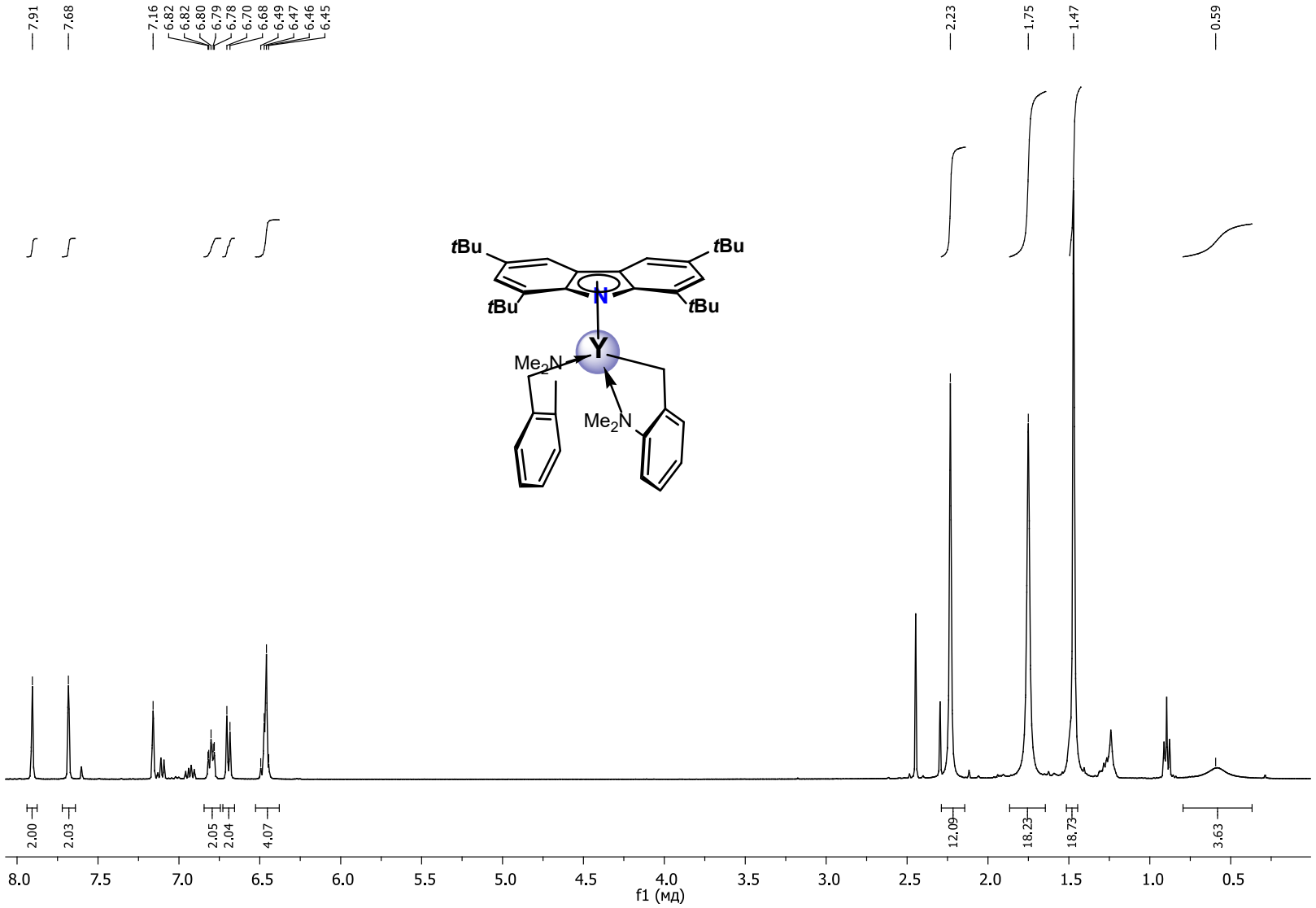

Figure S7. ^{1}H NMR spectrum of [*t*Bu$_4$Carb]Y(*o*-NMe$_2$C$_6$H$_5$CH$_2$)$_2$ (**2-Y**) (400 MHz, C$_6$D$_6$, 293 K).

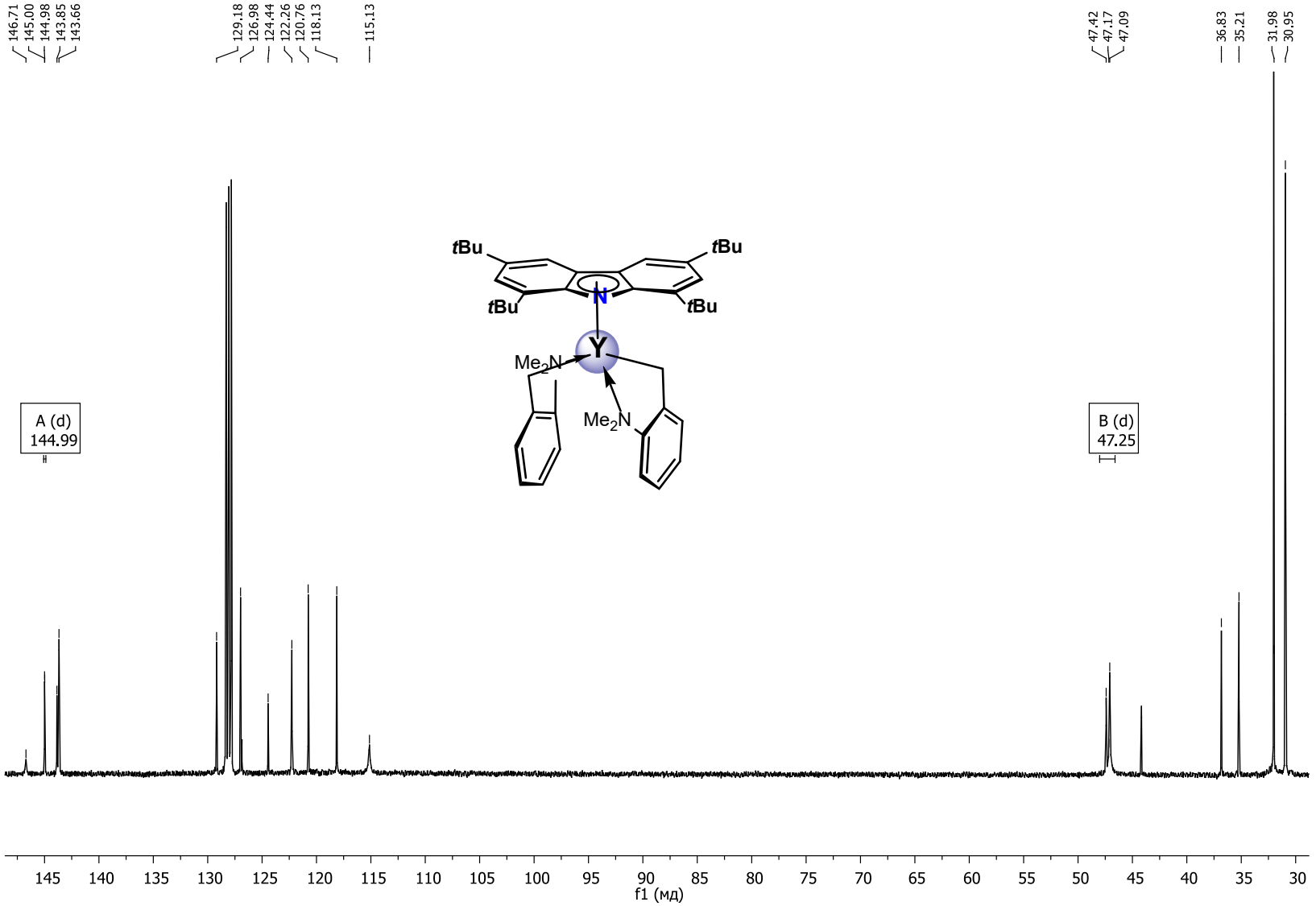

Figure S8. $^{13}C\{^{1}H\}$ NMR spectrum of [*t*Bu$_4$Carb]Y(*o*-NMe$_2$C$_6$H$_5$CH$_2$)$_2$ (**2-Y**) (100 MHz, C$_6$D$_6$, 293 K).

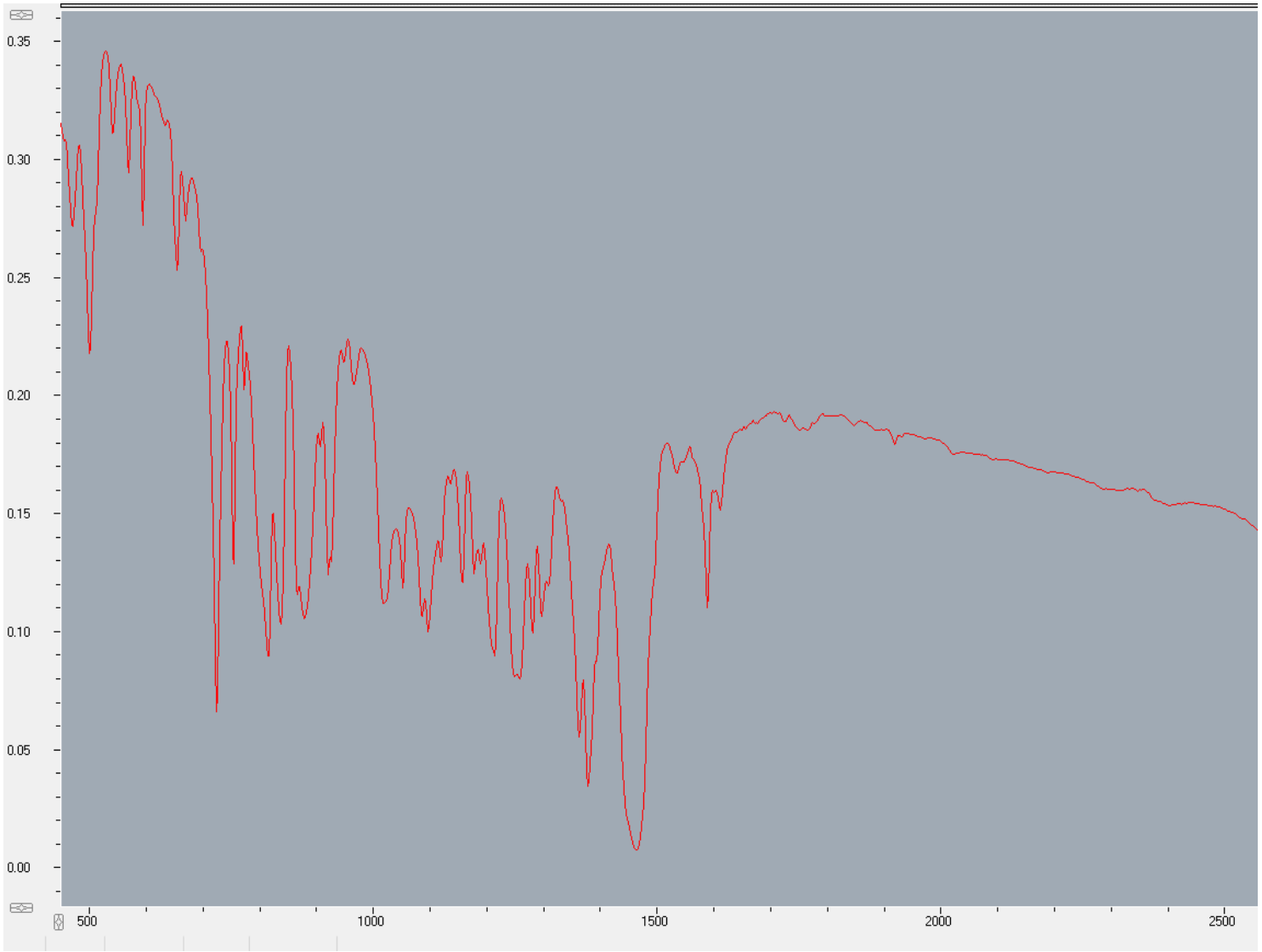

Figure S9. IR spectrum of complex [*t*Bu$_4$Carb]Y(*o*-NMe$_2$C$_6$H$_5$CH$_2$)$_2$ (**2-Y**) (KBr, Nujol mull).

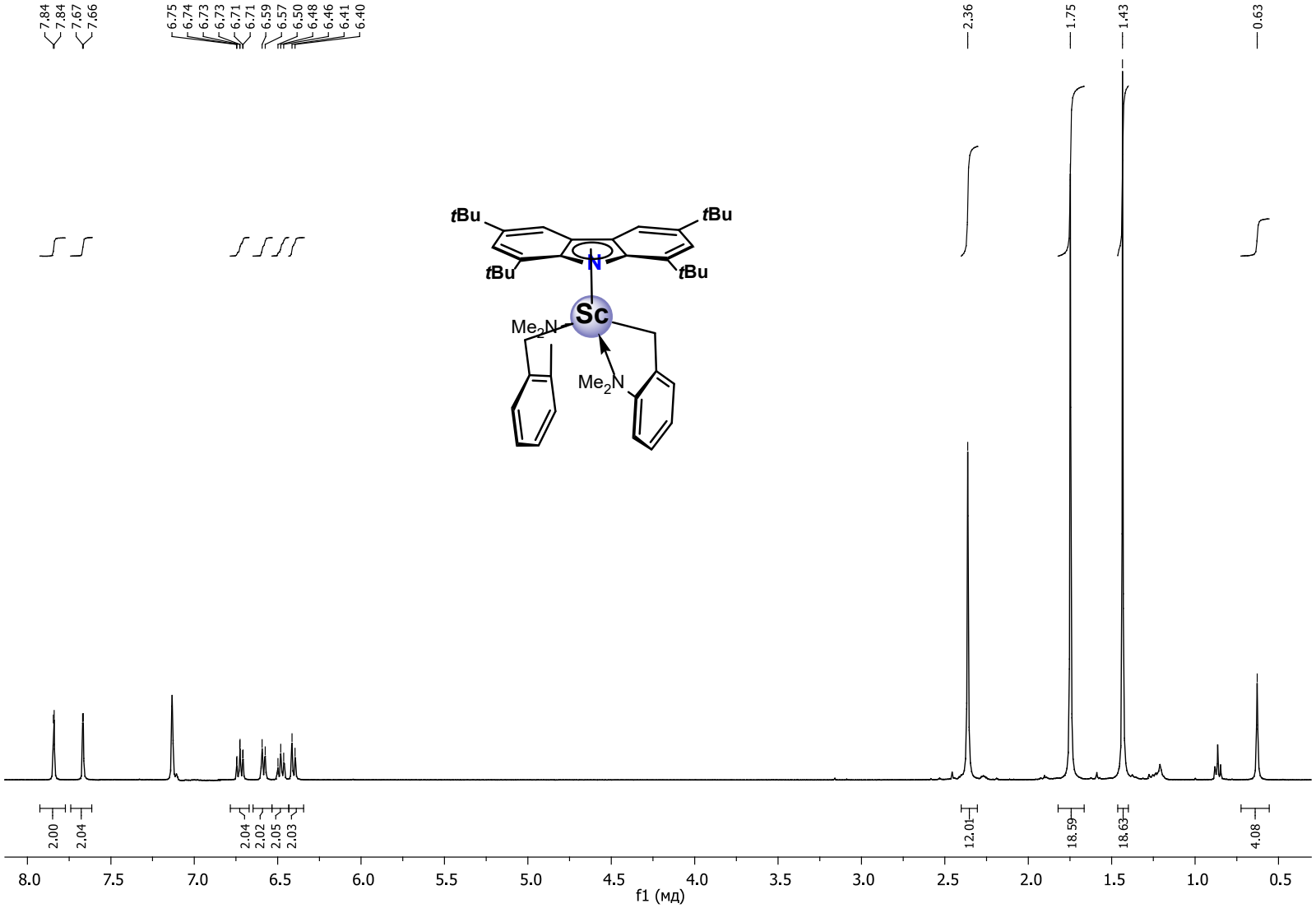

Figure S10. ^{1}H NMR spectrum of [*t*Bu$_4$Carb]Sc(*o*-NMe$_2$C$_6$H$_5$CH$_2$)$_2$ (**2-Sc**) (400 MHz, C$_6$D$_6$, 293 K).

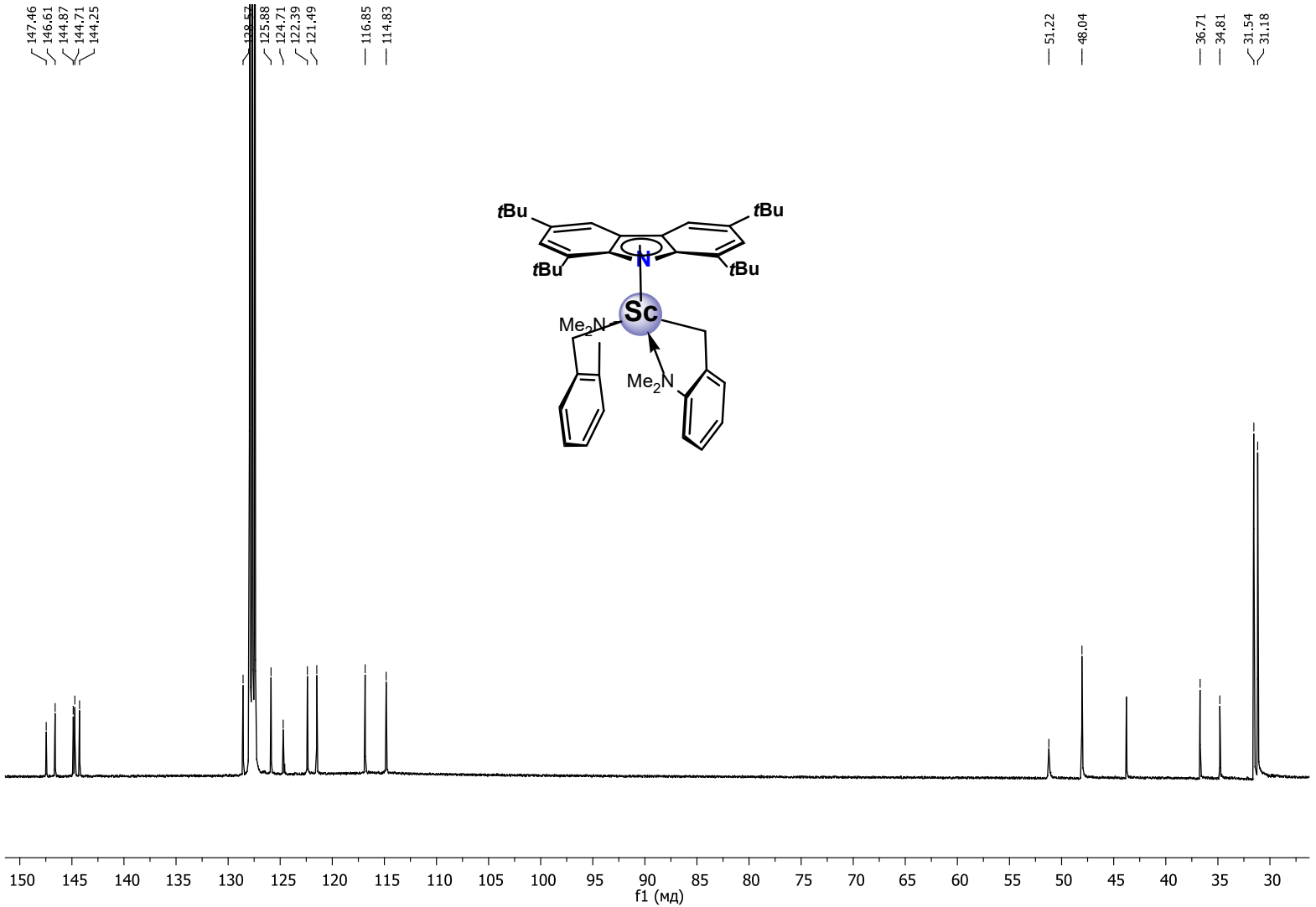

Figure S11. $^{13}C\{^{1}H\}$ NMR spectrum of [*t*Bu$_4$Carb]Sc(*o*-NMe$_2$C$_6$H$_5$CH$_2$)$_2$ (**2-Sc**) (100 MHz, C$_6$D$_6$, 293 K).

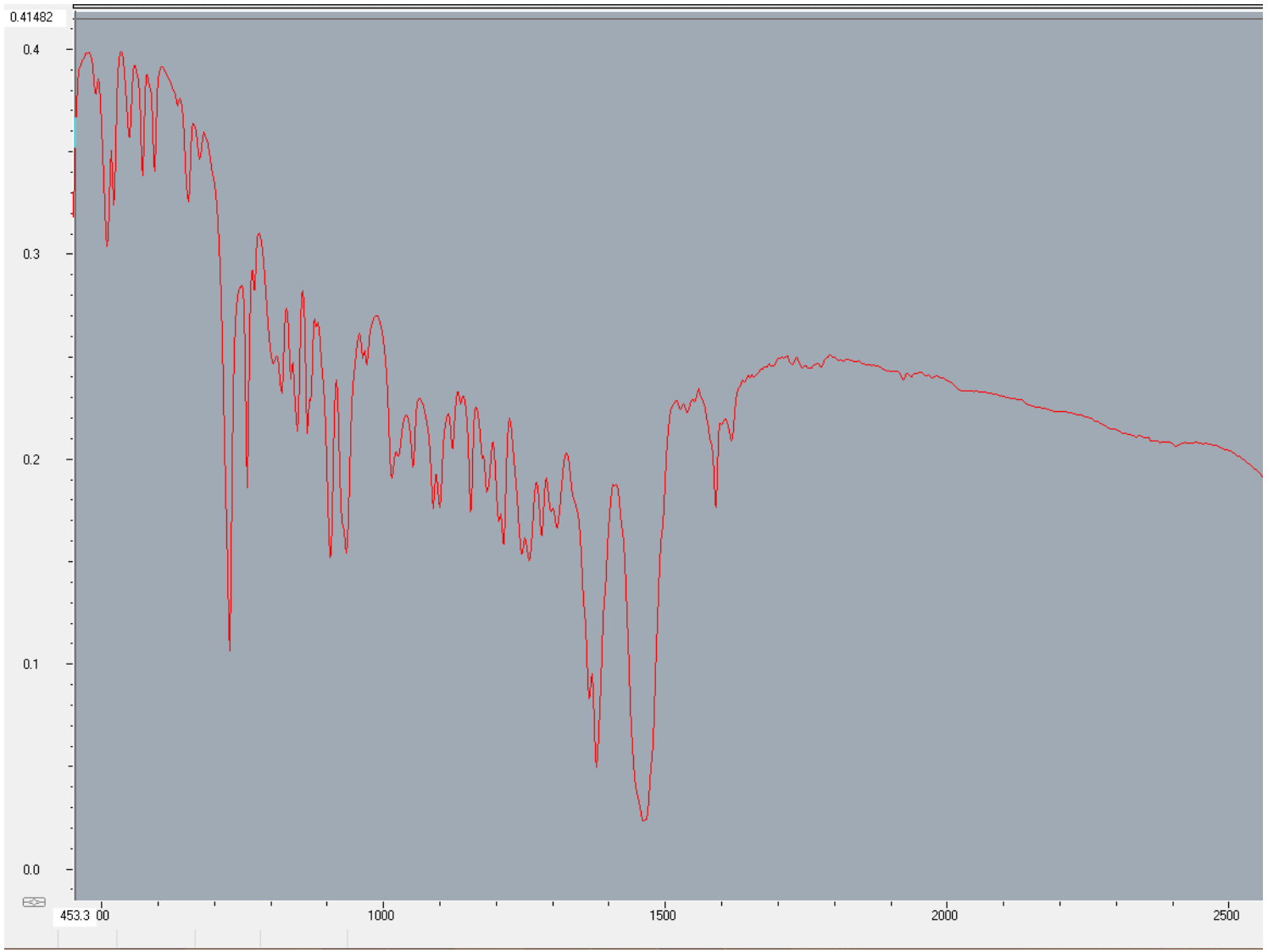

Figure S12. IR spectrum of complex [*t*Bu$_4$Carb]Sc(*o*-NMe$_2$C$_6$H$_5$CH$_2$)$_2$ (**2-Sc**) (KBr, Nujol mull).

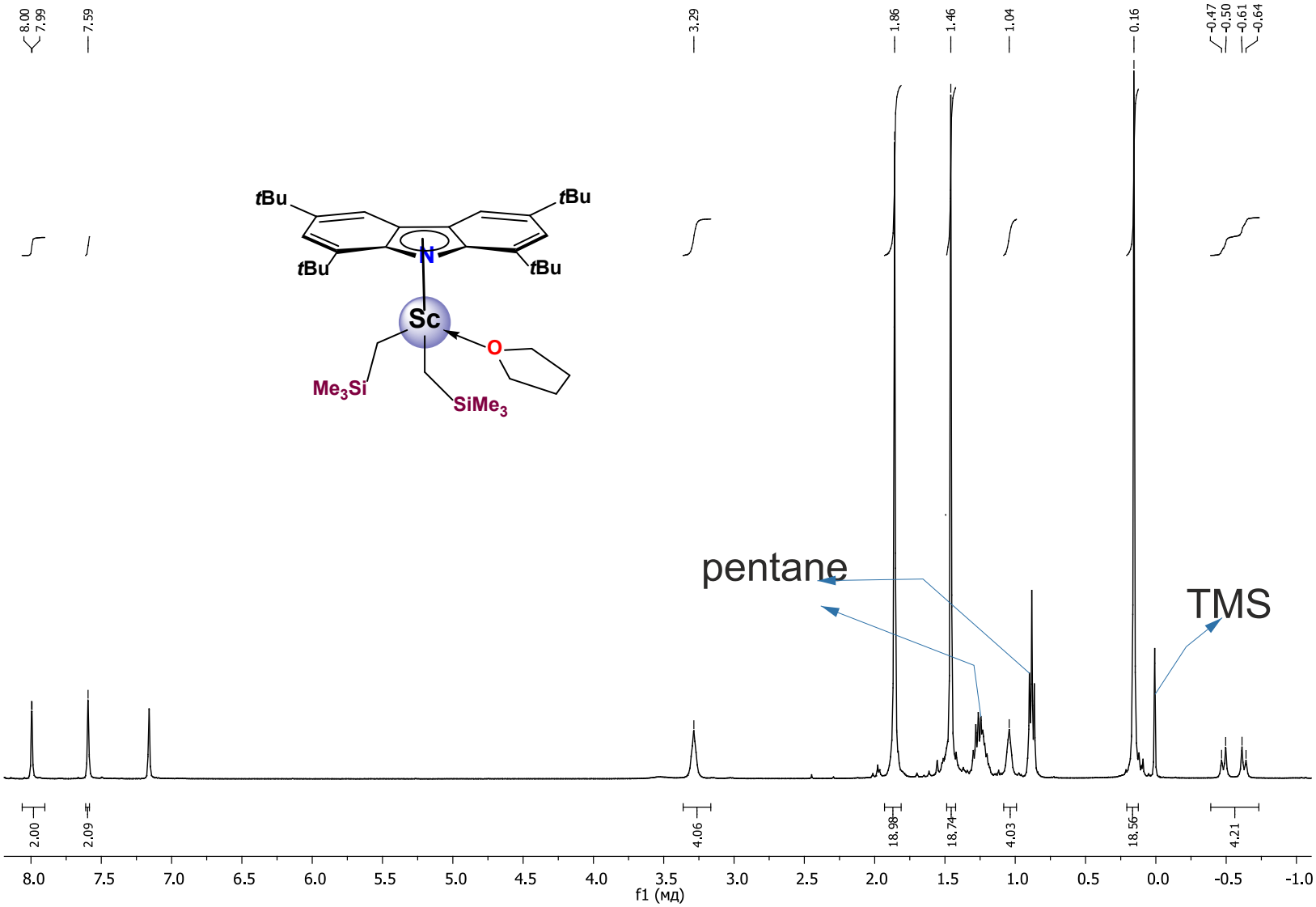

Figure S13. ^{1}H NMR spectrum of [*t*Bu$_4$Carb]Sc(CH$_2$SiMe$_3$)$_2$(THF) (**3-Sc**) (400 MHz, C$_6$D$_6$, 293 K).

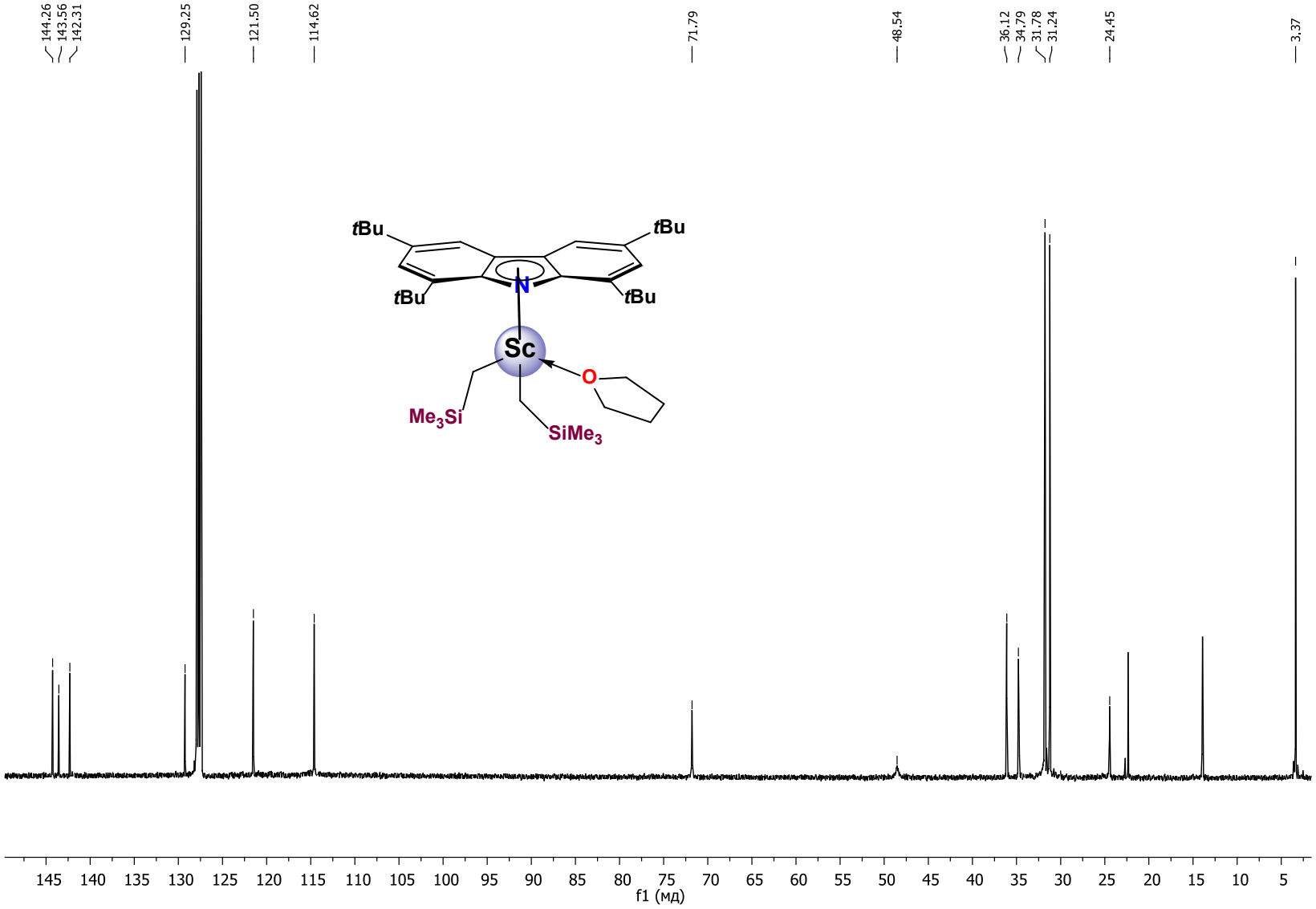

Figure S14. $^{13}C\{^{1}H\}$ NMR spectrum of [*t*Bu$_4$Carb]Sc(CH$_2$SiMe$_3$)$_2$(THF) (**3-Sc**) (100 MHz, C_6D_6, 293 K).

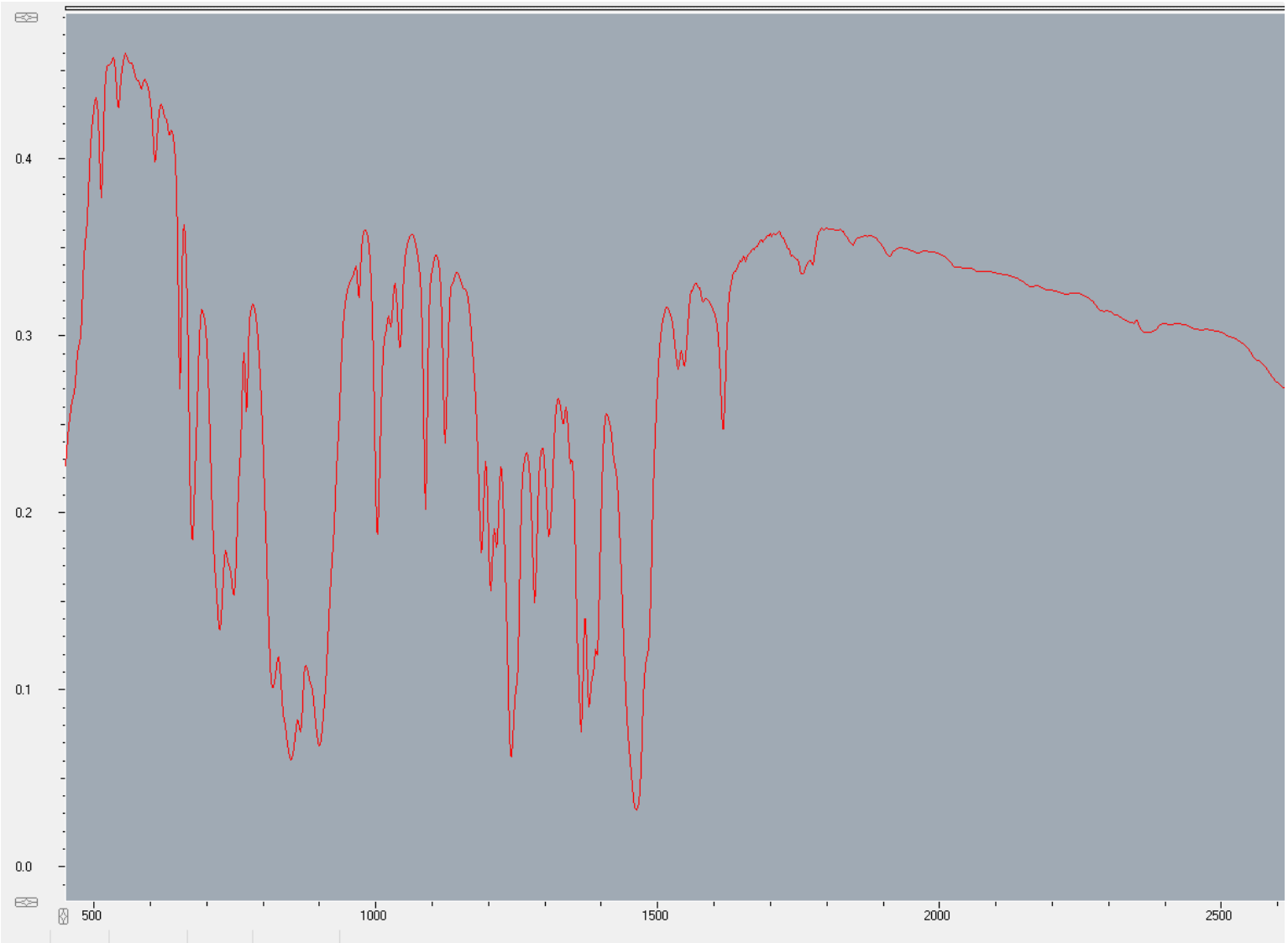

Figure S15. IR spectrum of complex [*t*Bu$_4$Carb]Sc(CH$_2$SiMe$_3$)$_2$(THF) (**3-Sc**) (KBr, Nujol mull).

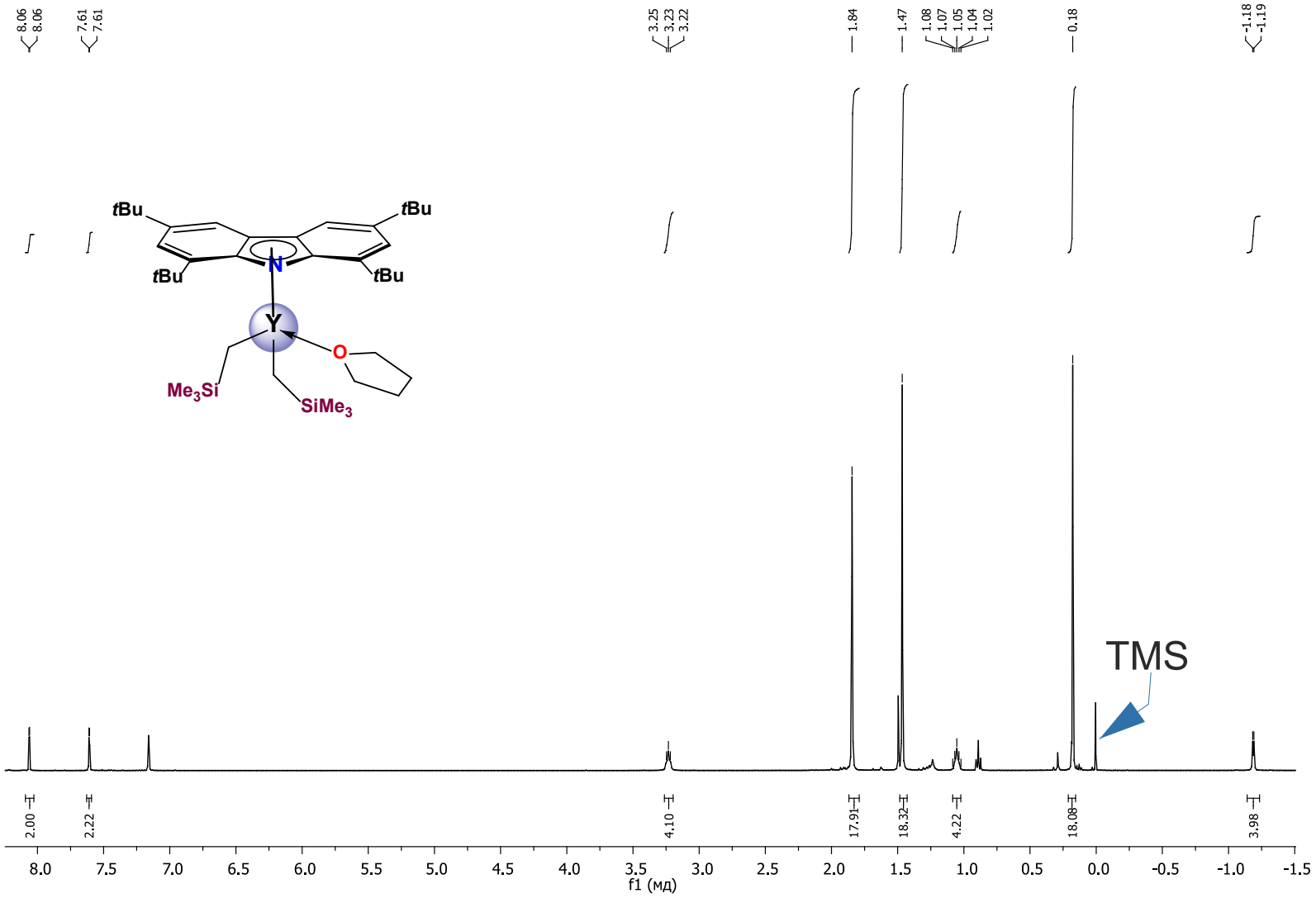

Figure S16. ^{1}H NMR spectrum of [*t*Bu$_4$Carb]Y(CH$_2$SiMe$_3$)$_2$(THF) (**3-Y**) (400 MHz, C$_6$D$_6$, 293 K).

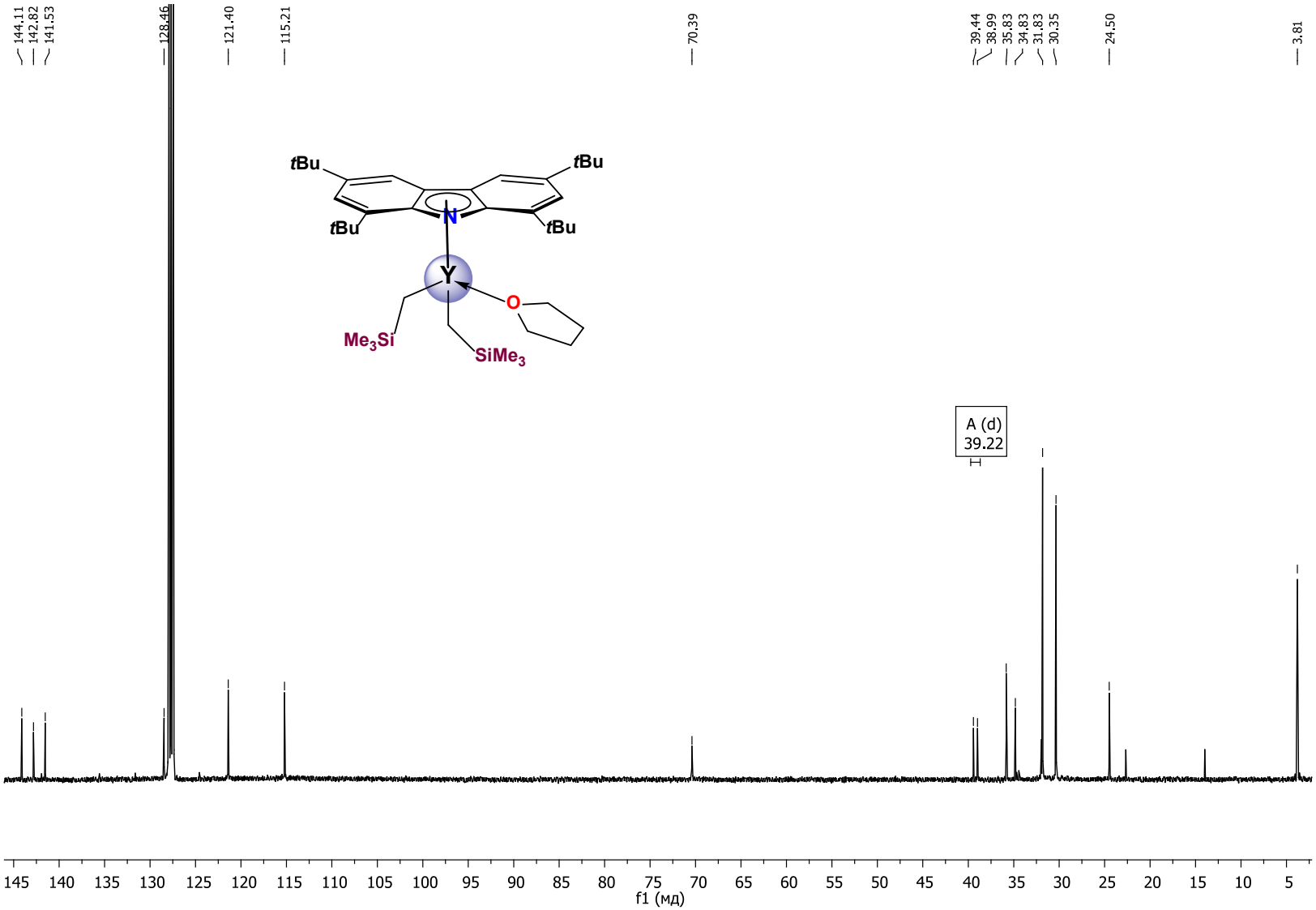

Figure S17. $^{13}C\{^{1}H\}$ NMR spectrum of [*t*Bu$_4$Carb]Y(CH$_2$SiMe$_3$)$_2$(THF) (**3-Y**) (100 MHz, C_6D_6, 298 K).

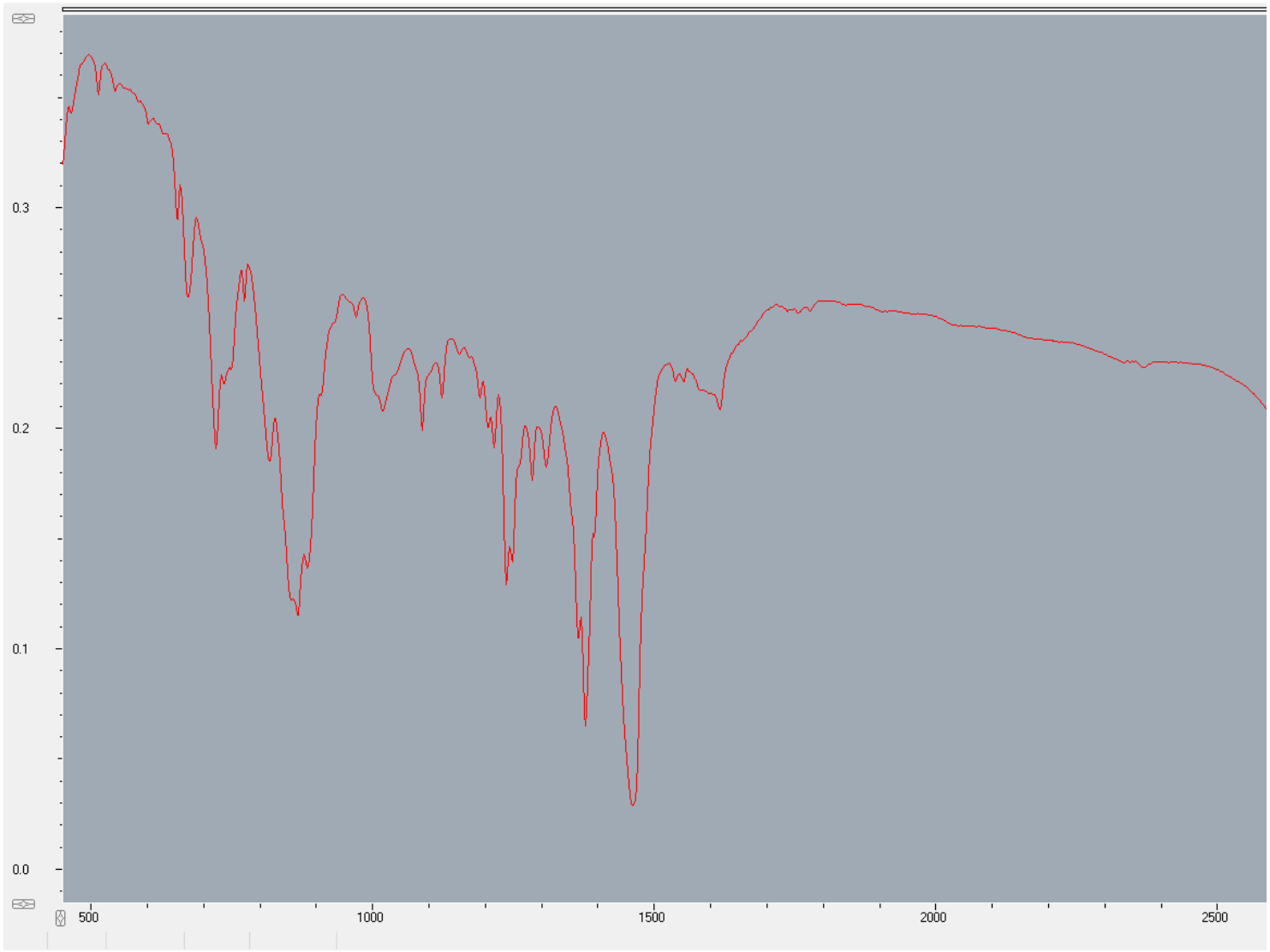

Figure S18. IR spectrum of complex [*t*Bu$_4$Carb]Y(CH$_2$SiMe$_3$)$_2$(THF) (**3-Y**) (KBr, Nujol mull).

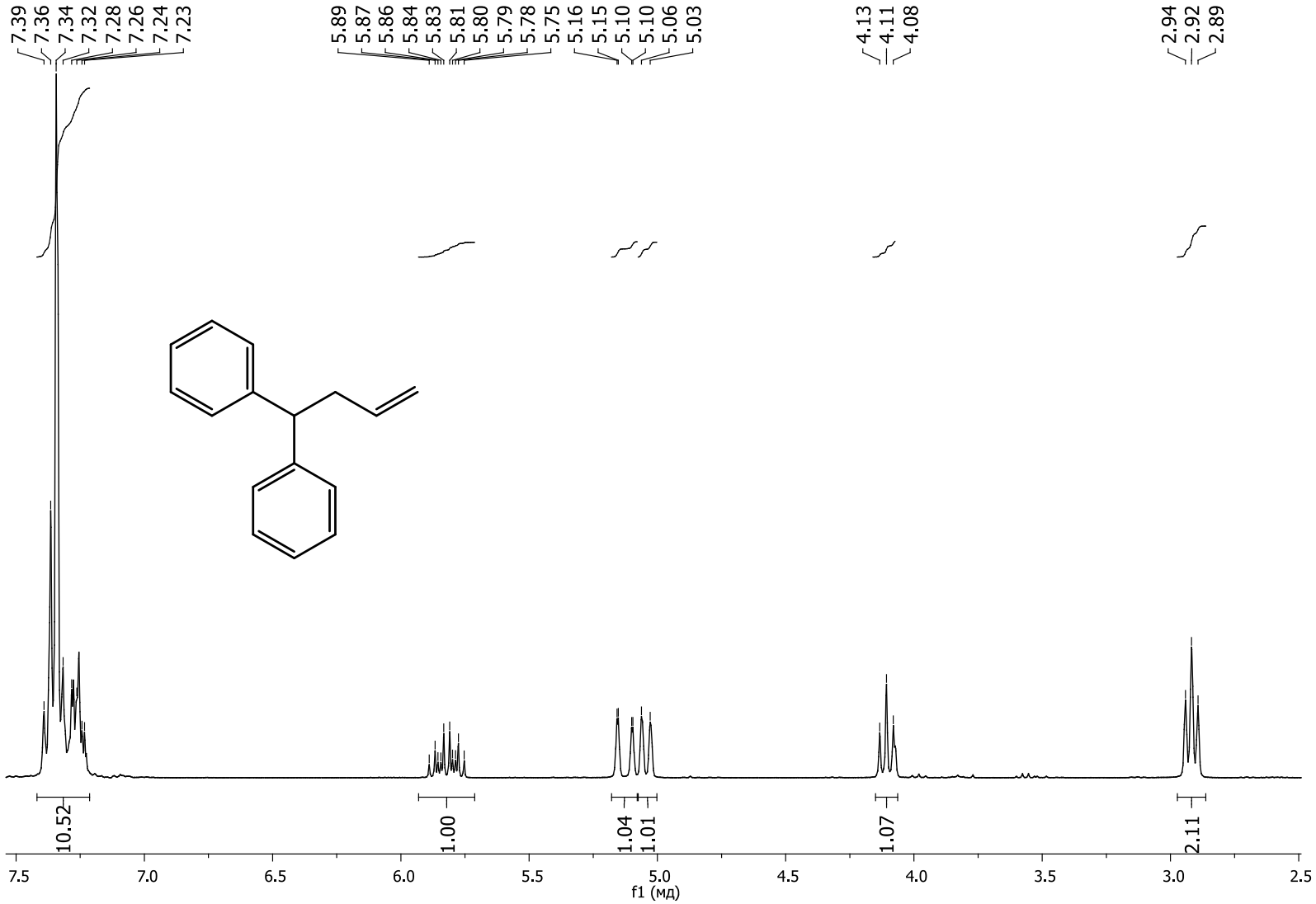

Figure S19. ^{1}H NMR spectrum of 4,4-diphenyl-but-1-ene (300 MHz, $CDCl_3$, 300 K).

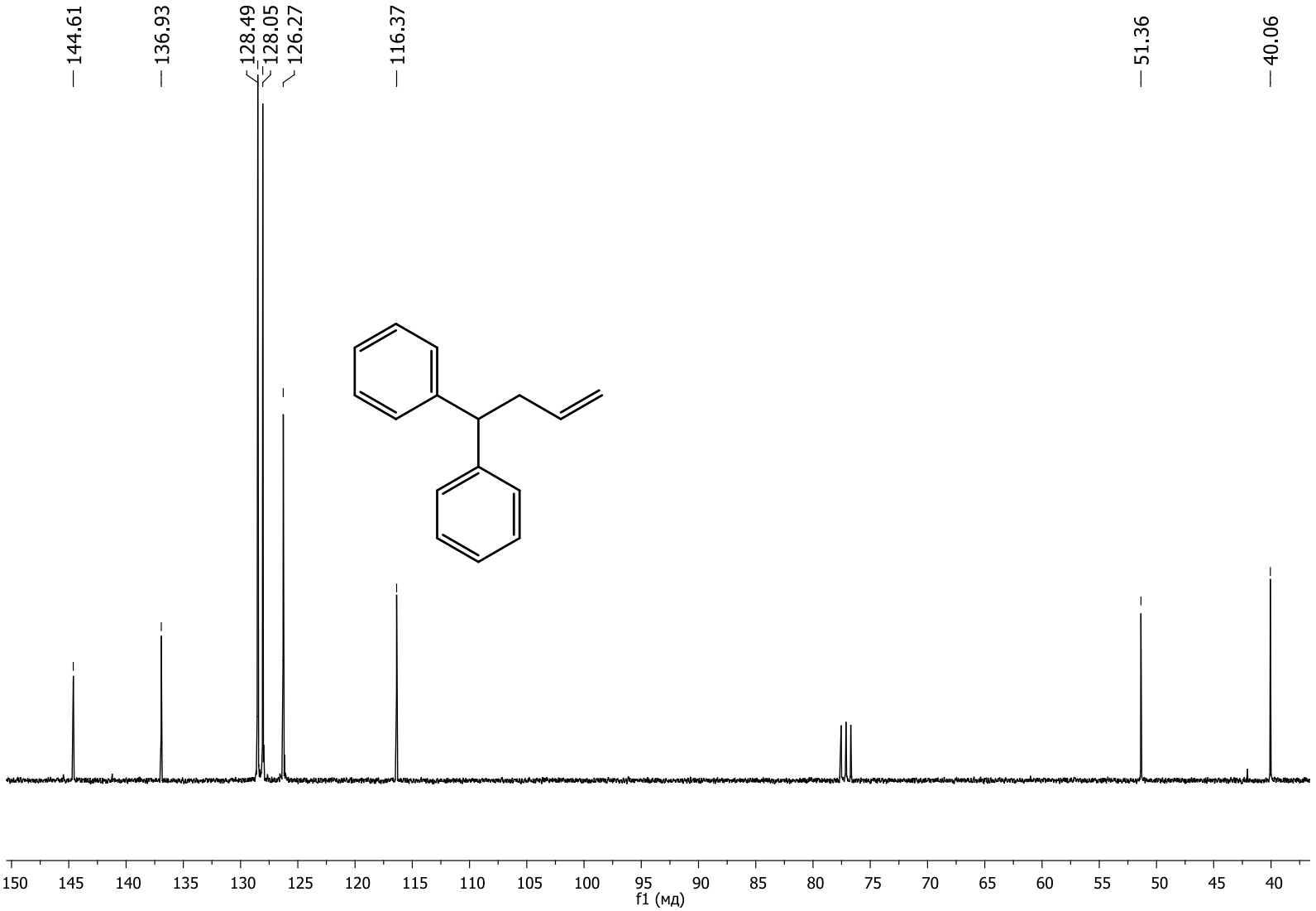

Figure S20. $^{13}C\{^{1}H\}$ NMR spectrum of 4,4-diphenyl-but-1-ene (75 MHz, $CDCl_3$, 300 K).

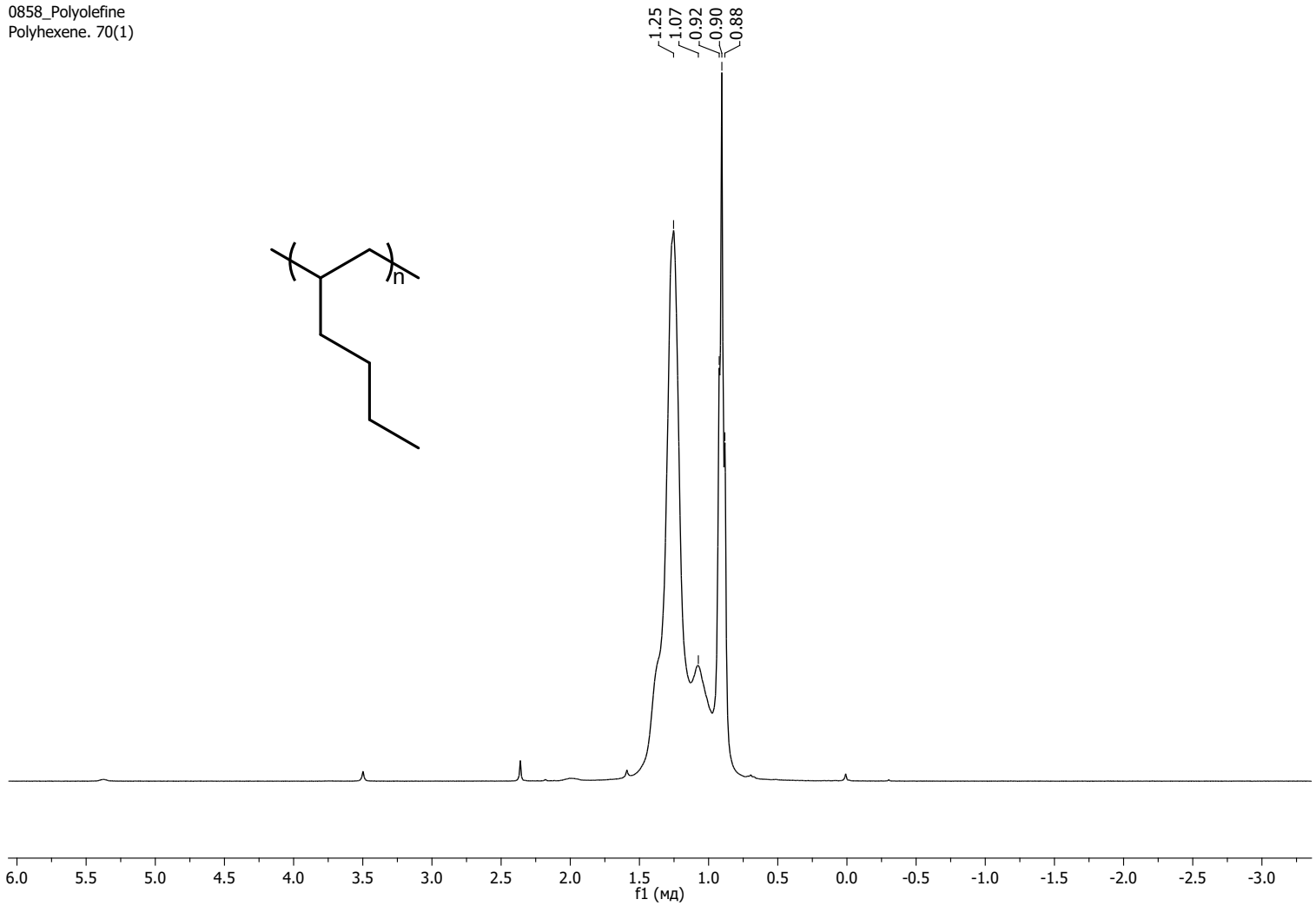

Figure S21. ^{1}H NMR spectrum of poly(1-hexene) (300 MHz, $CDCl_3$, 300 K).

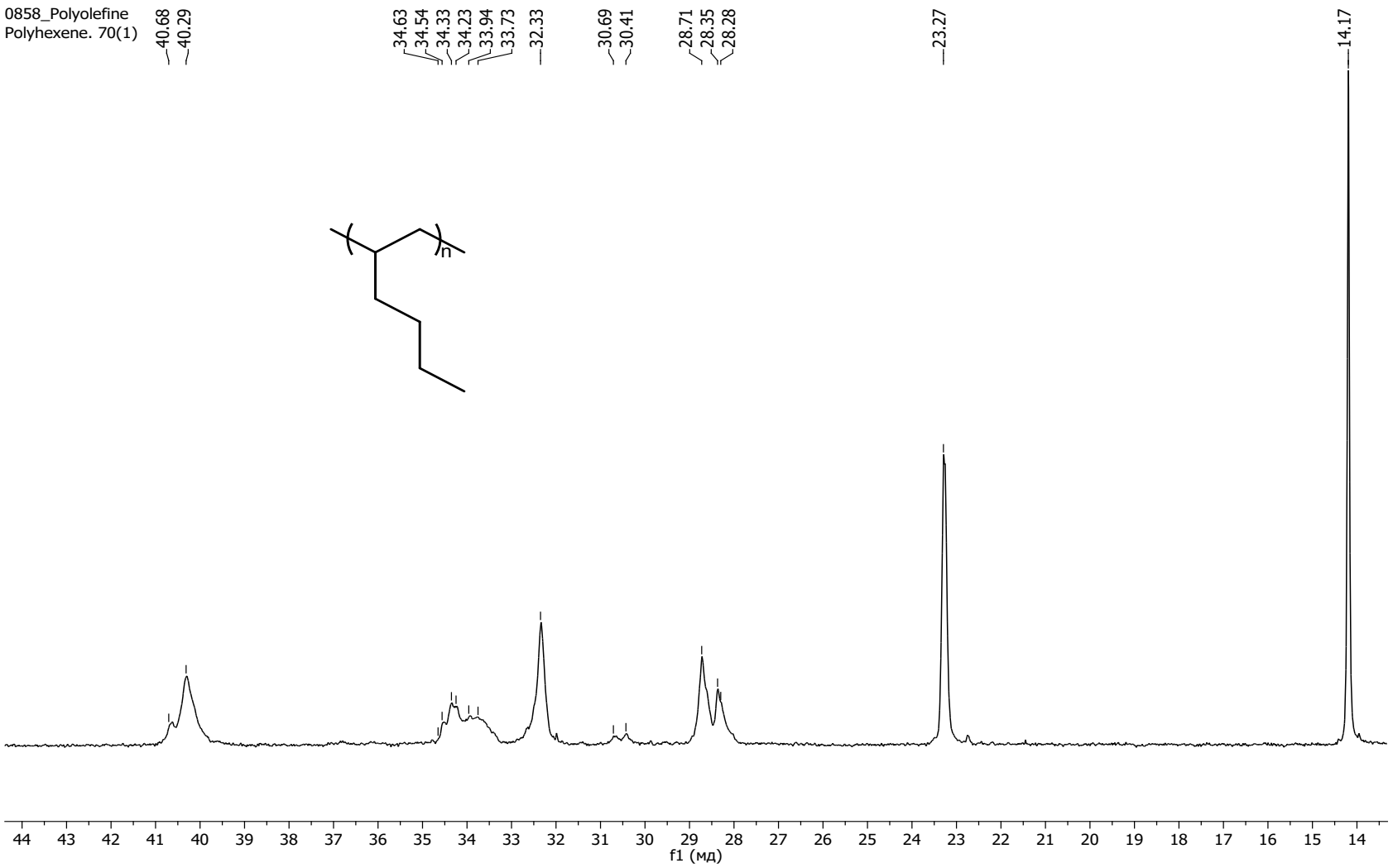

Figure S22. $^{13}C\{^{1}H\}$ NMR spectrum of poly(1-hexene) (75 MHz, $CDCl_3$, 300 K).

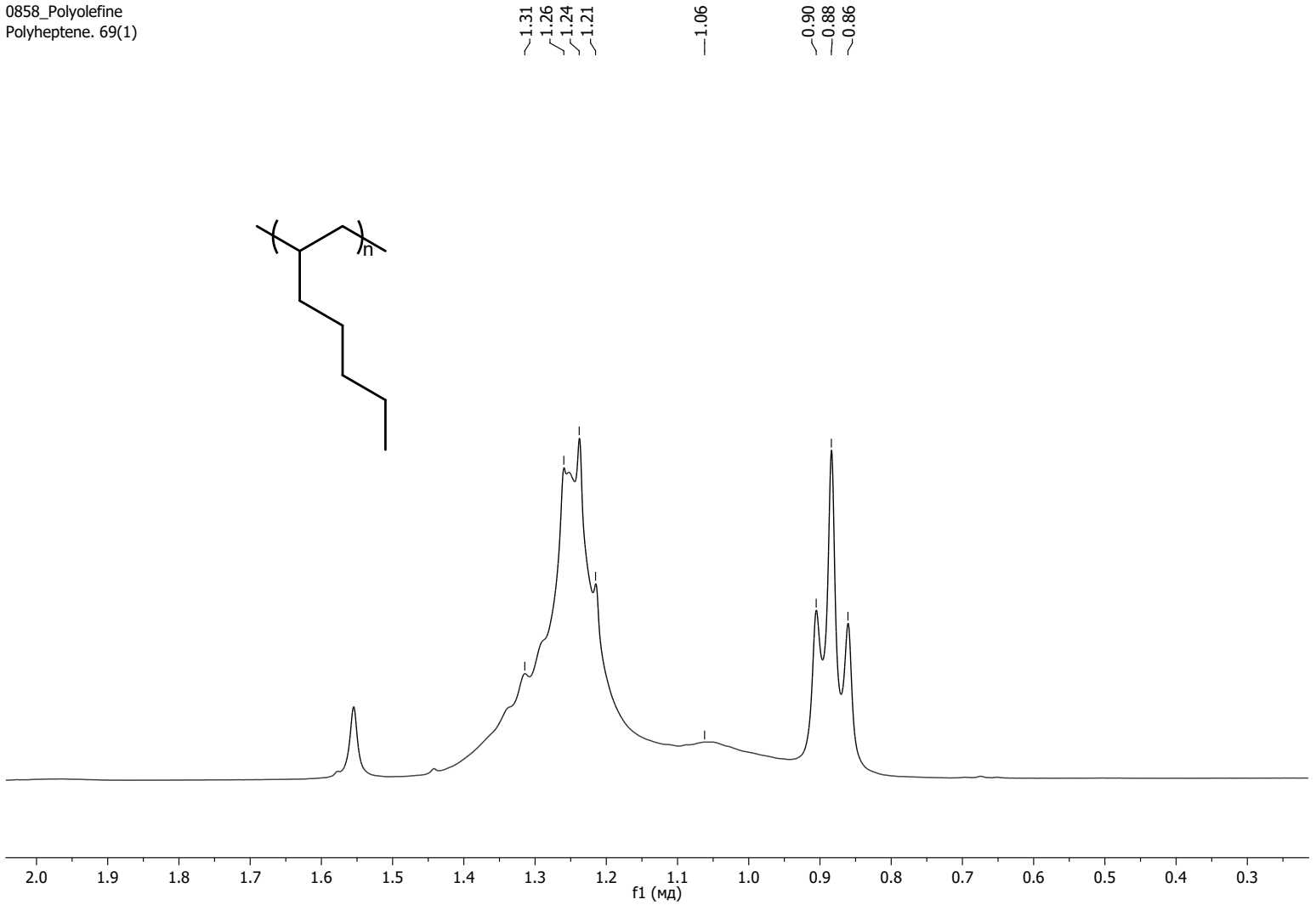

Figure S23. ^{1}H NMR spectrum of poly(1-heptene) (300 MHz, $CDCl_3$, 300 K).

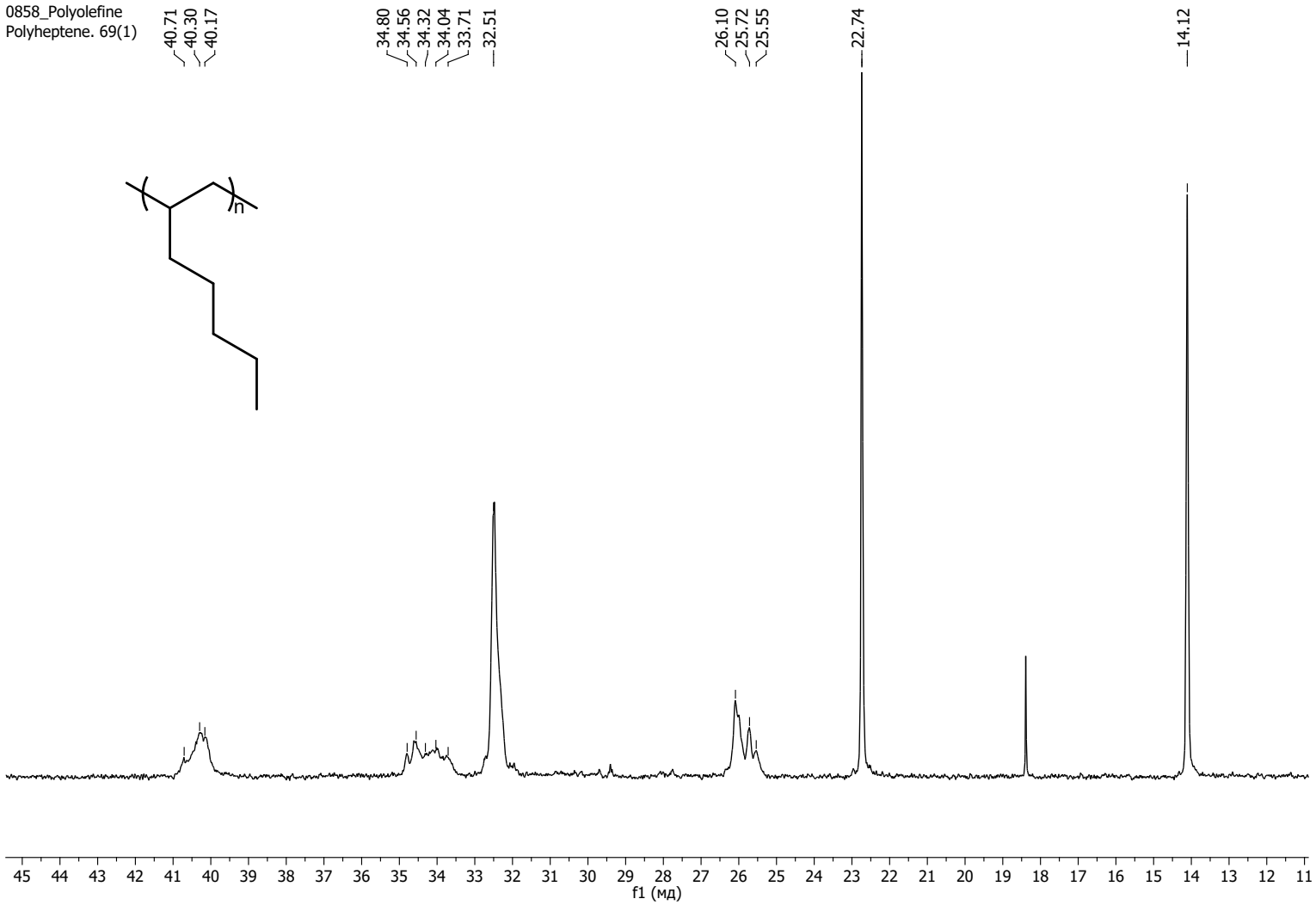

Figure S24. $^{13}C\{^{1}H\}$ NMR spectrum of poly(1-heptene) (75 MHz, $CDCl_3$, 300 K).

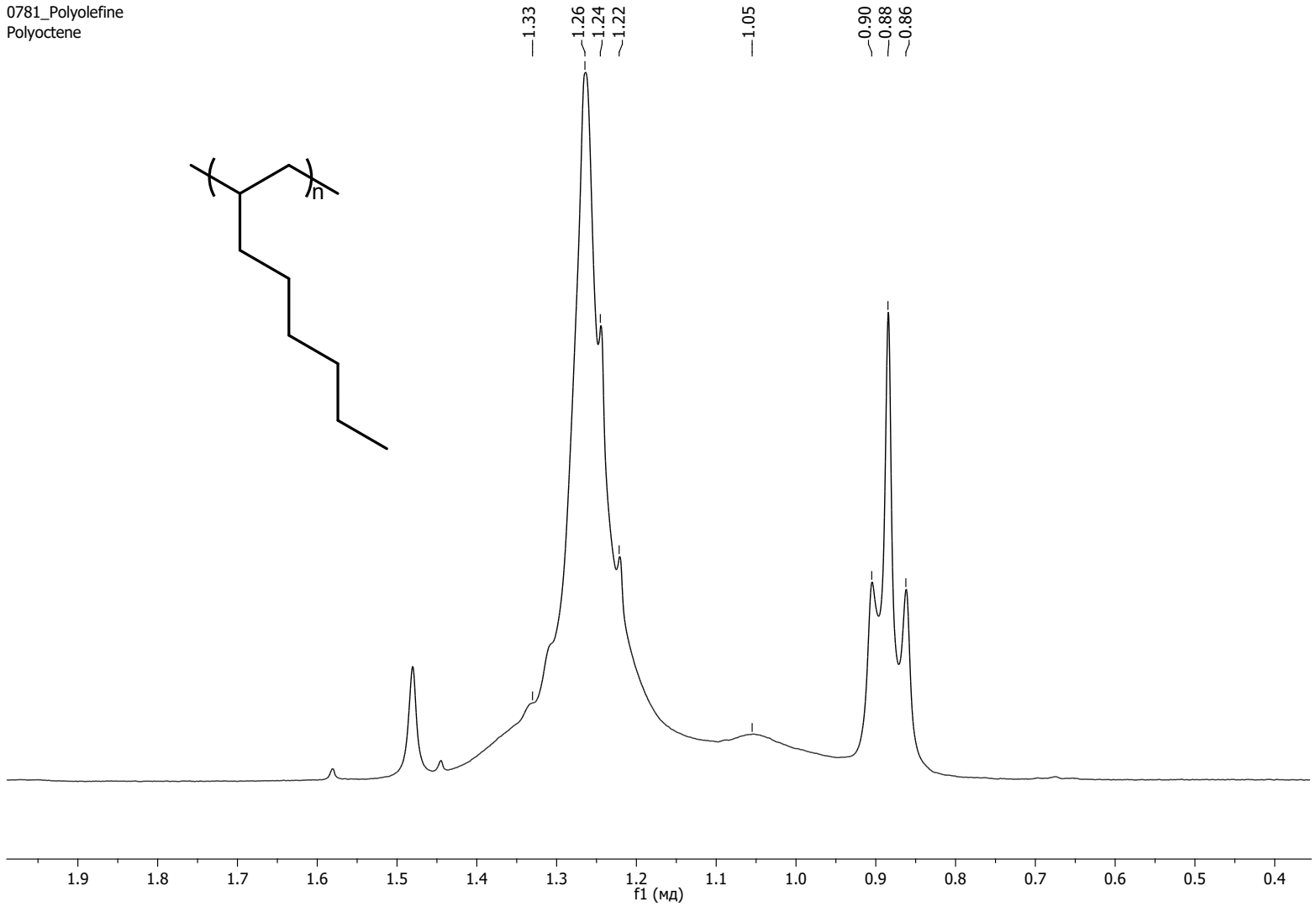

Figure S25. ^{1}H NMR spectrum of poly(1-octene) (300 MHz, $CDCl_3$, 300 K).

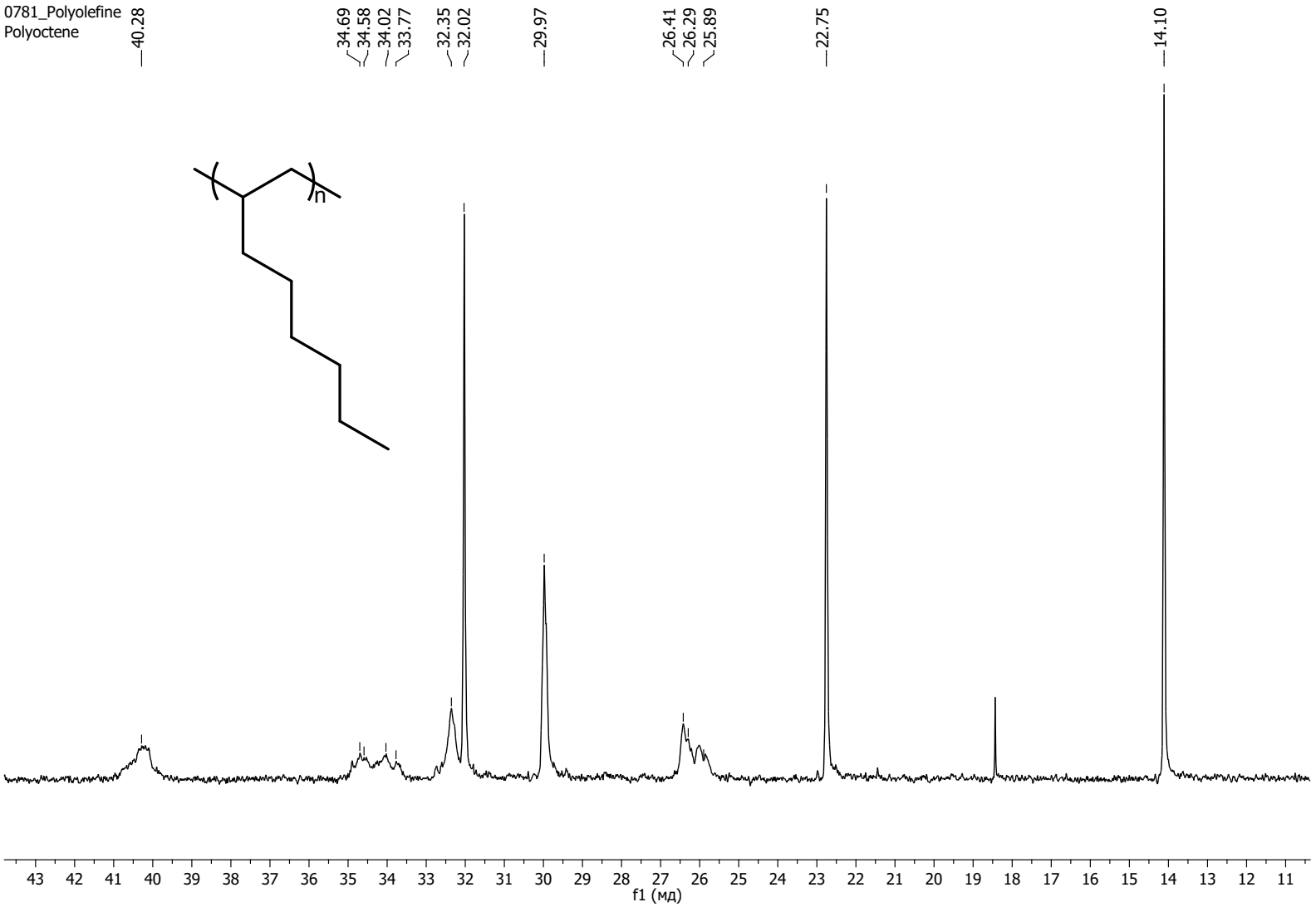

Figure S26. $^{13}C\{^{1}H\}$ NMR spectrum of poly(1-octene) (75 MHz, $CDCl_3$, 300 K).

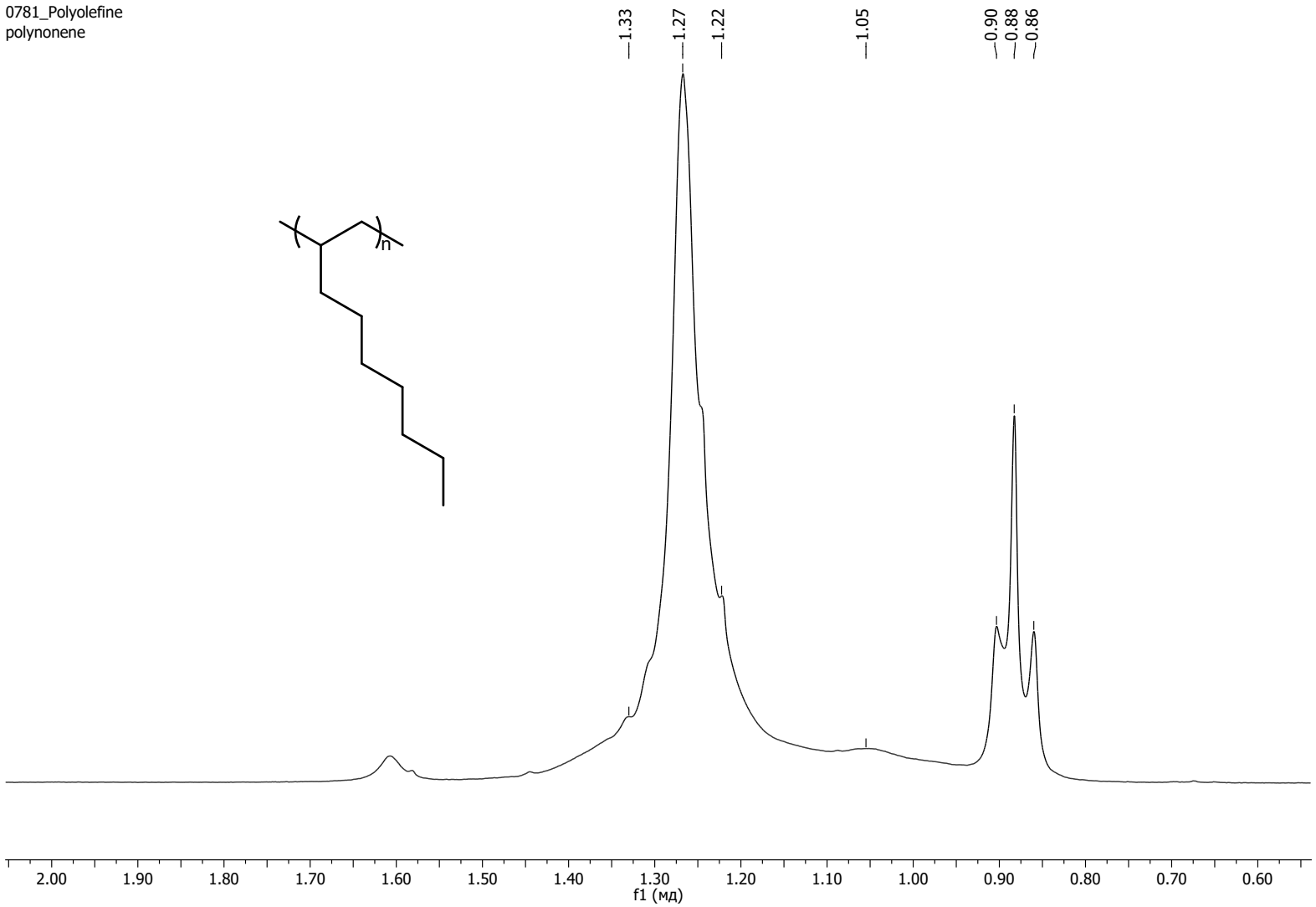

Figure S27. ^{1}H NMR spectrum of poly(1-nonene) (300 MHz, $CDCl_3$, 300 K).

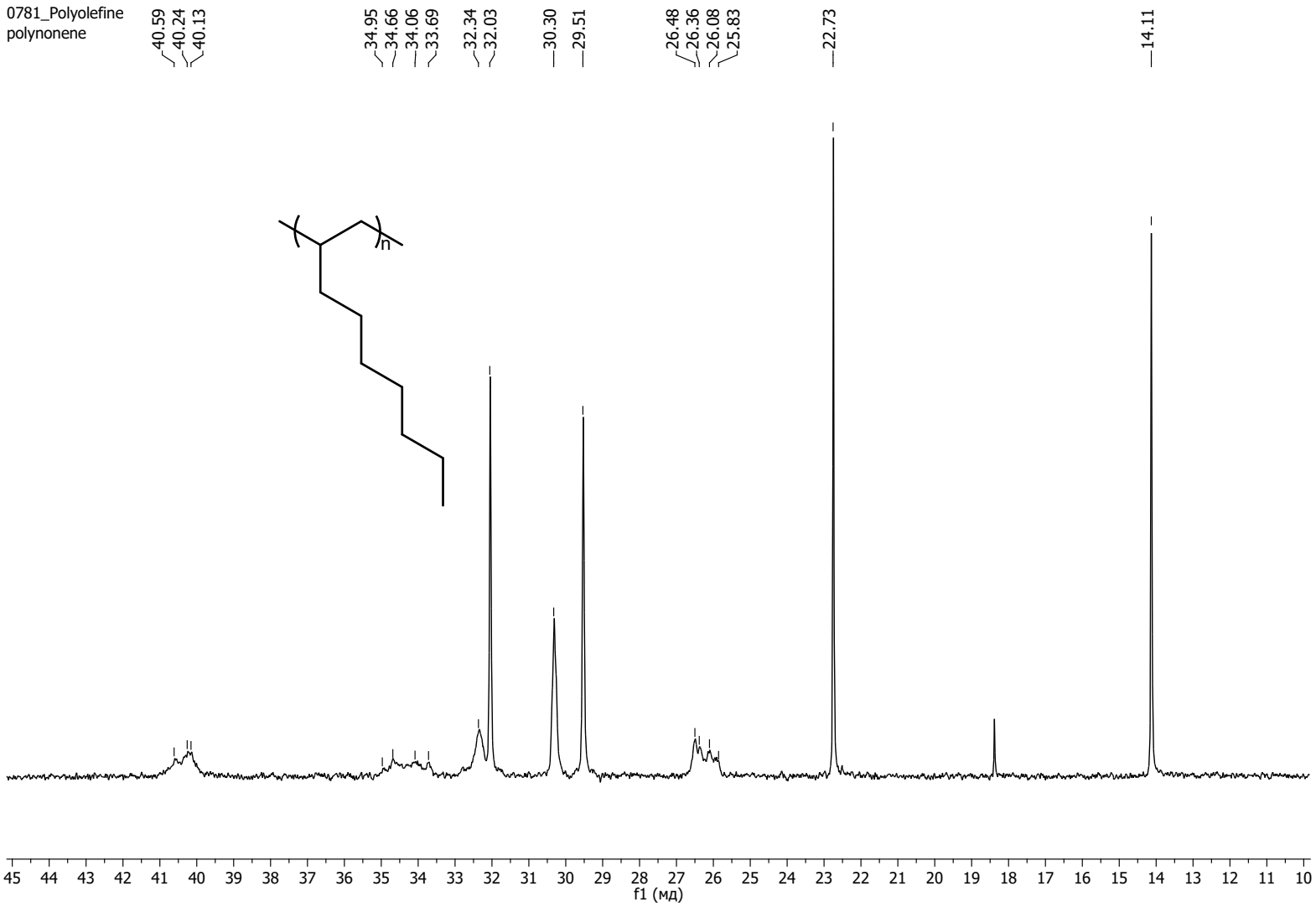

Figure S28. $^{13}C\{^{1}H\}$ NMR spectrum of poly(1-nonene) (75 MHz, $CDCl_3$, 300 K).

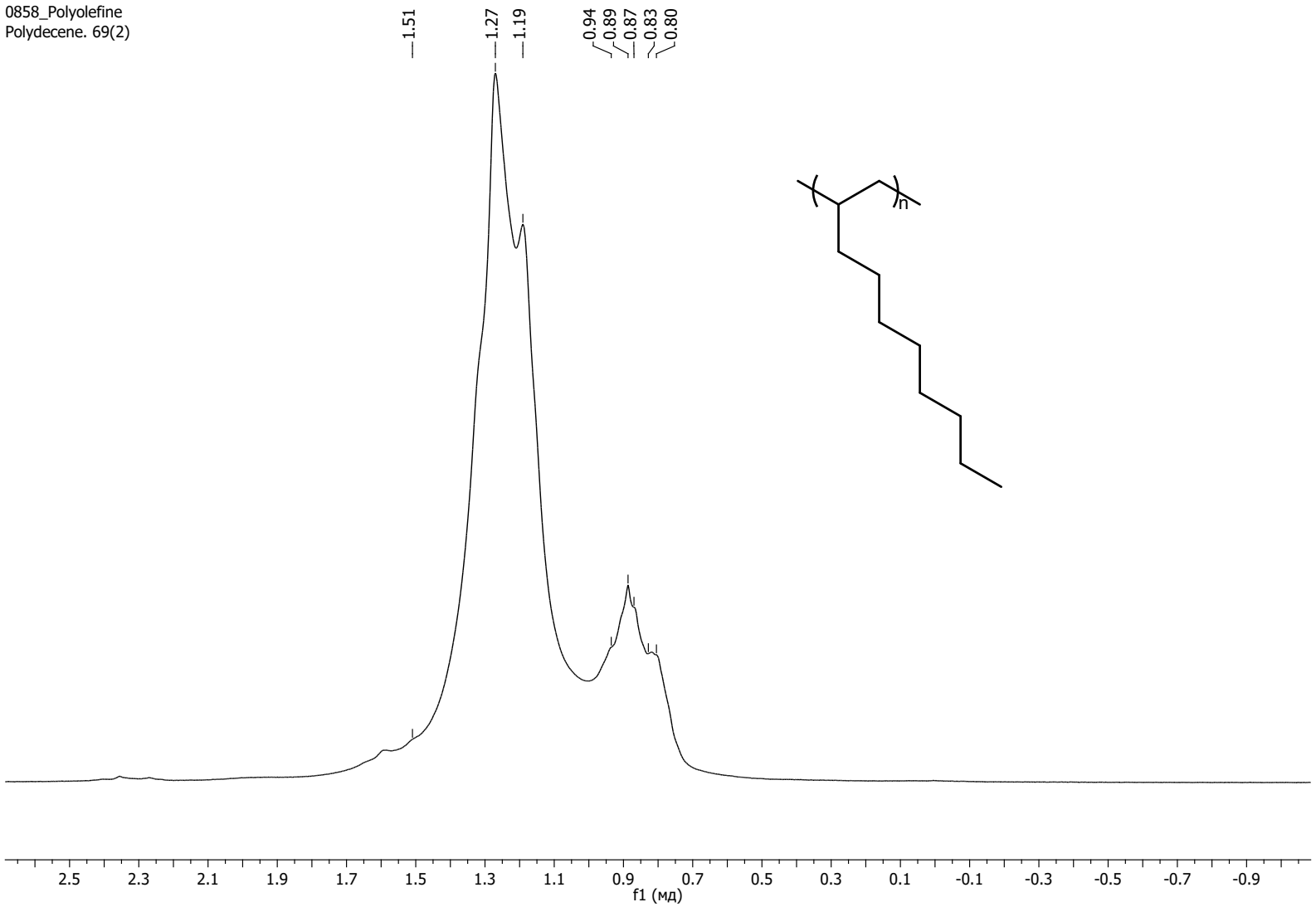

Figure S29. ^{1}H NMR spectrum of poly(1-decene) (300 MHz, $CDCl_3$, 300 K).

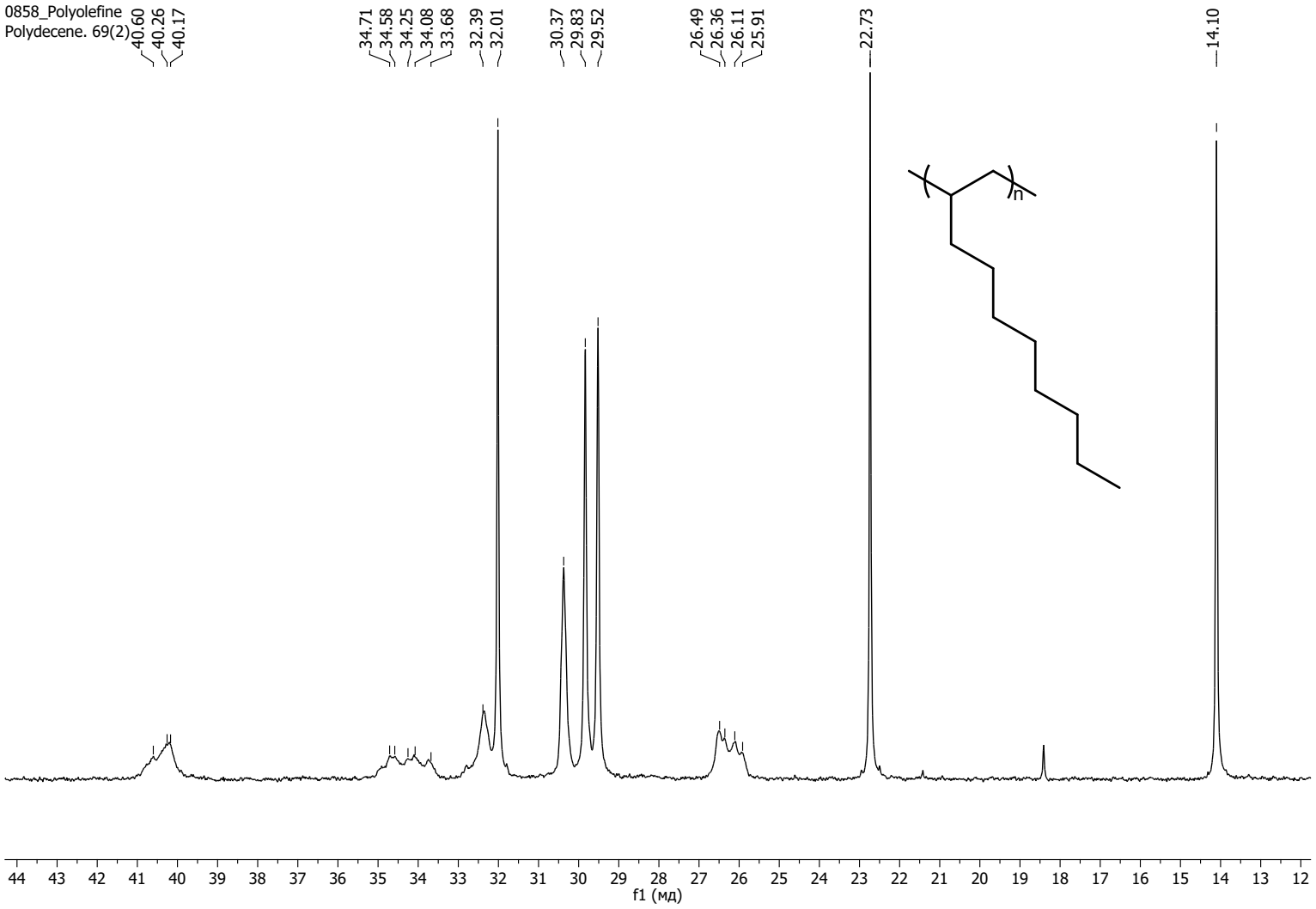

Figure S30. $^{13}C\{^{1}H\}$ NMR spectrum of poly(1-decene) (75 MHz, $CDCl_3$, 300 K).

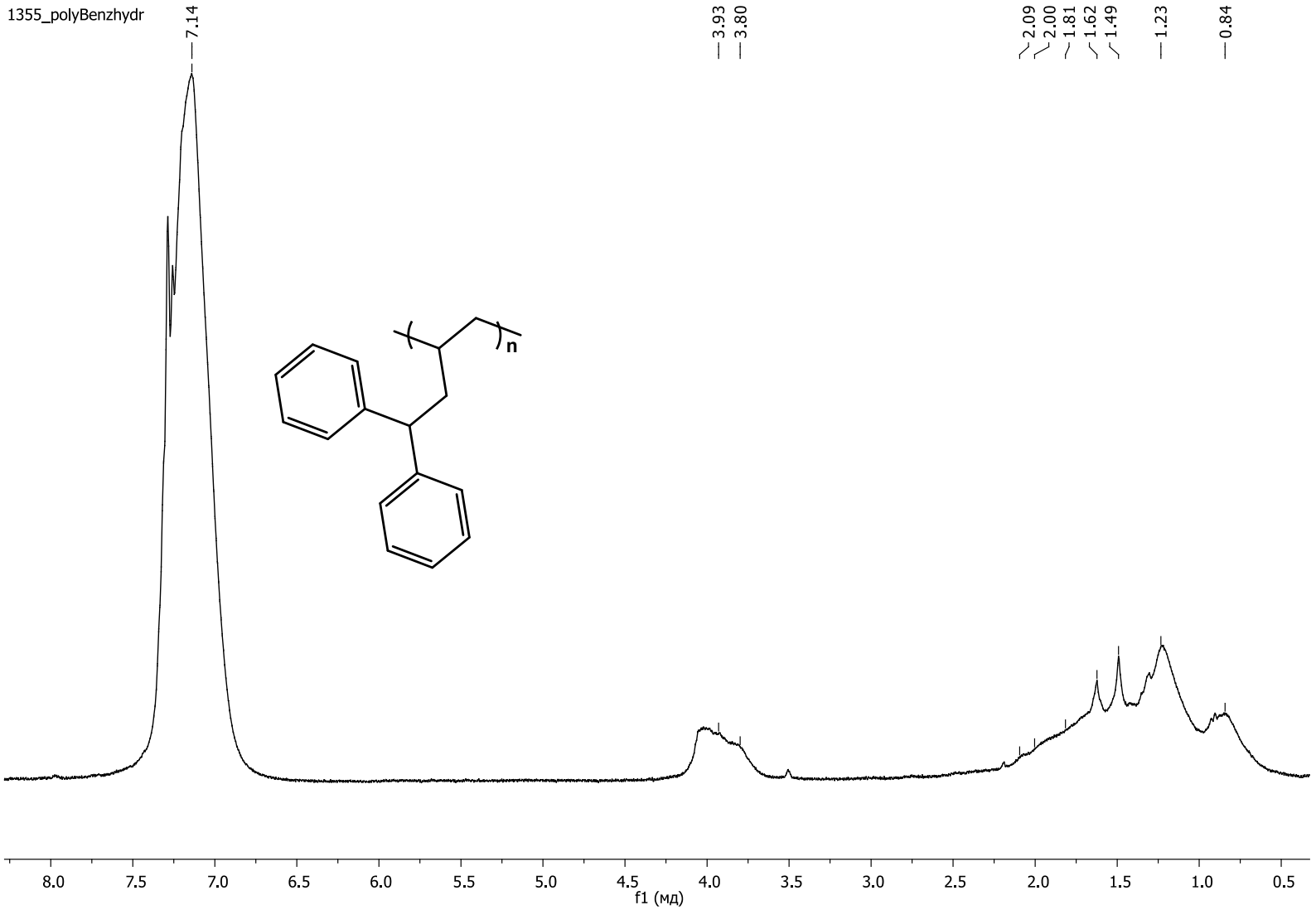

Figure S31. ^{1}H NMR spectrum of poly(4,4-diphenyl-but-1-ene) (300 MHz, $CDCl_3$, 300 K).

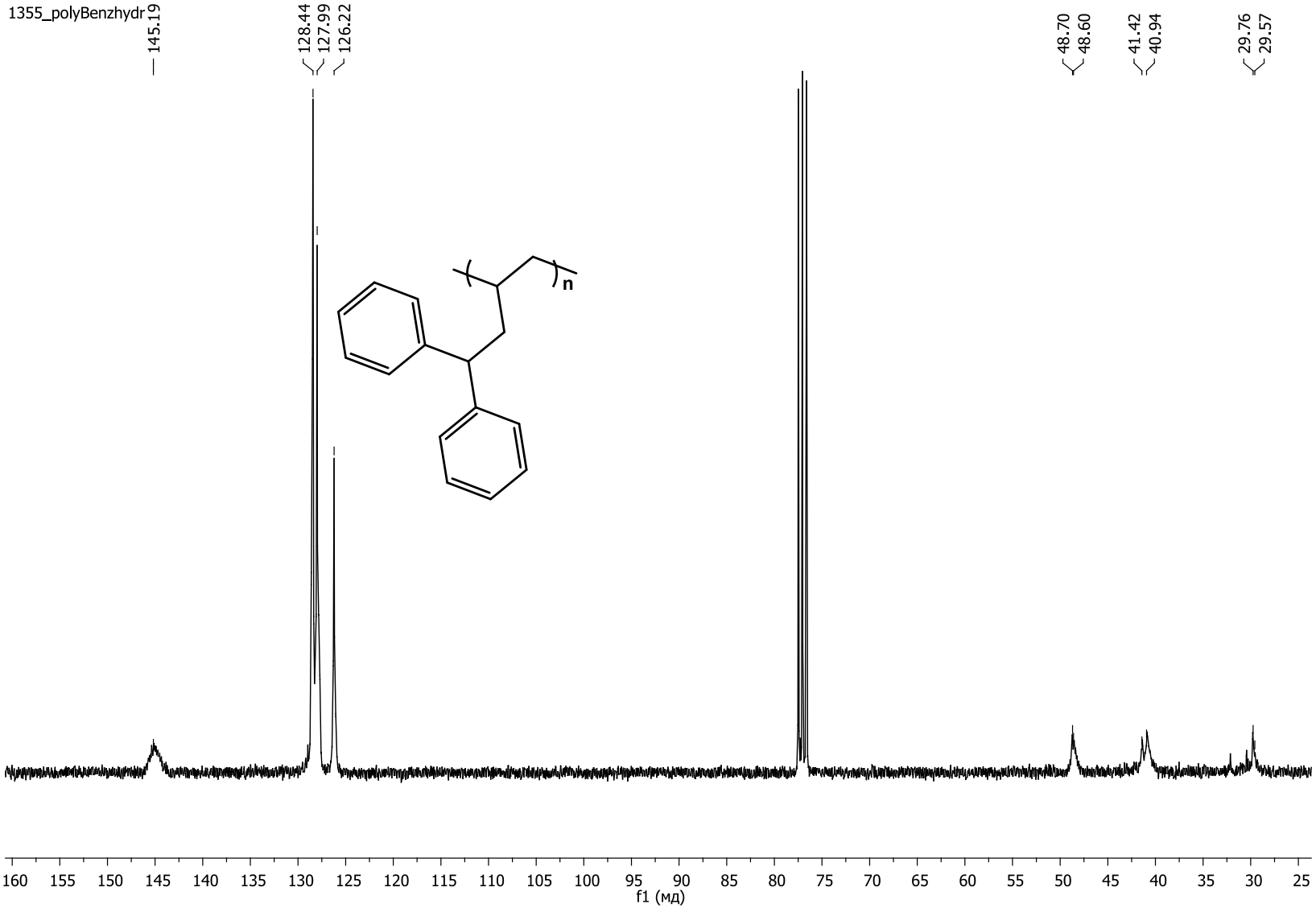

Figure S32. $^{13}C\{^{1}H\}$ NMR spectrum of poly(4,4-diphenyl-but-1-ene) (75 MHz, $CDCl_3$, 300 K).

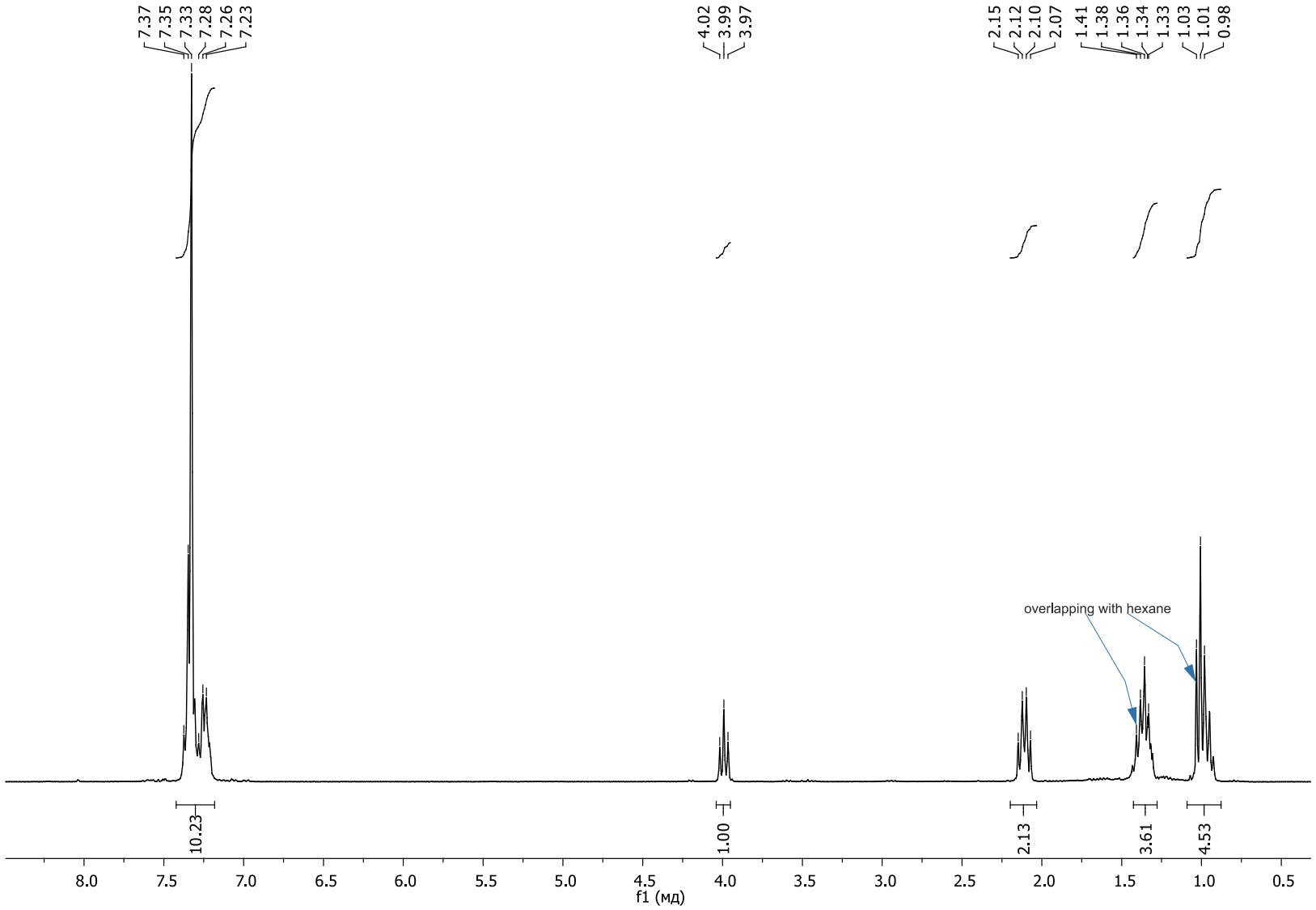

Figure S33. ^{1}H NMR spectrum of 1,1-diphenylbutane (300 MHz, $CDCl_3$, 300 K).

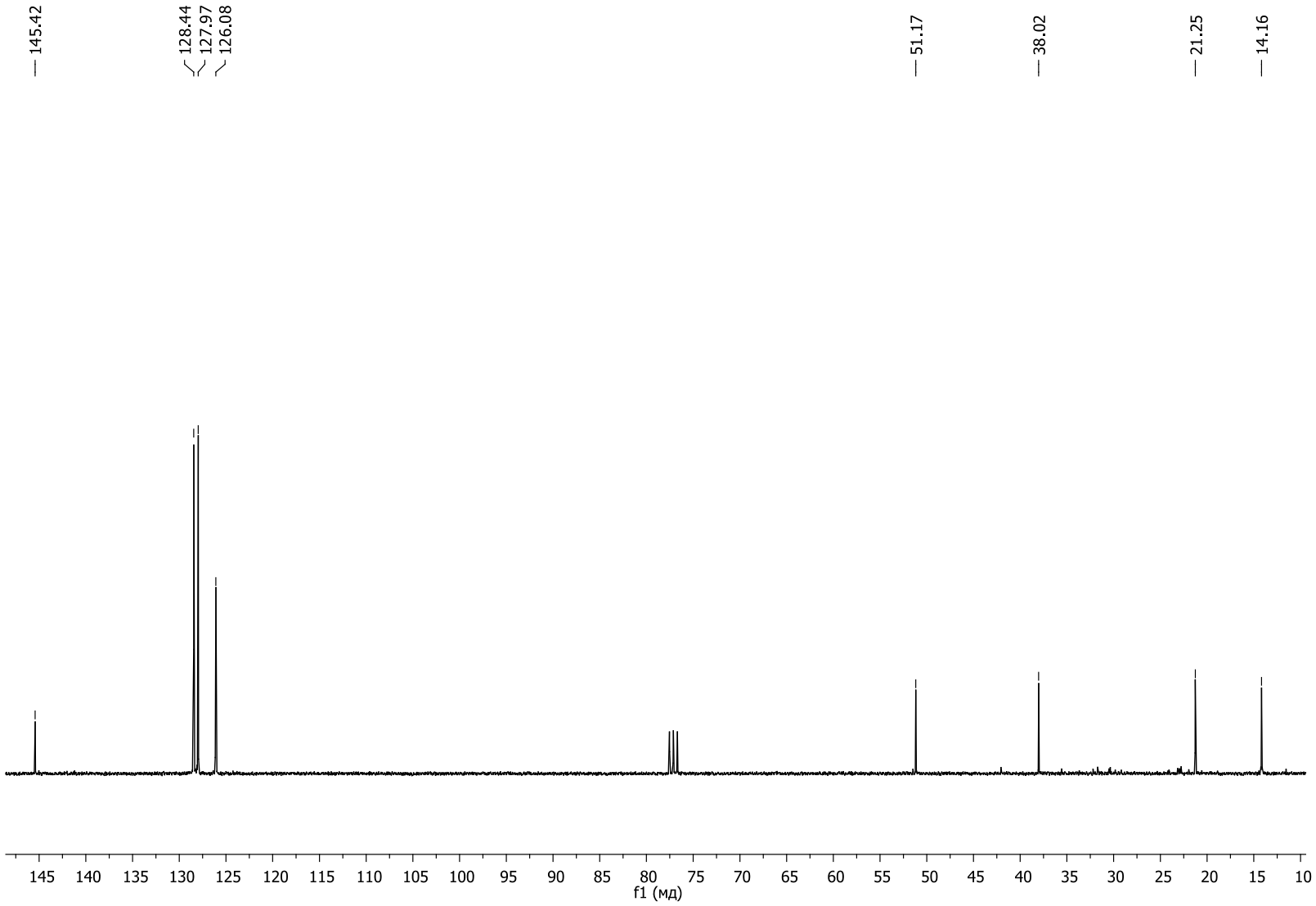

Figure S34. $^{13}C\{^{1}H\}$ NMR spectrum of 1,1-diphenylbutane (75 MHz, $CDCl_3$, 300 K).

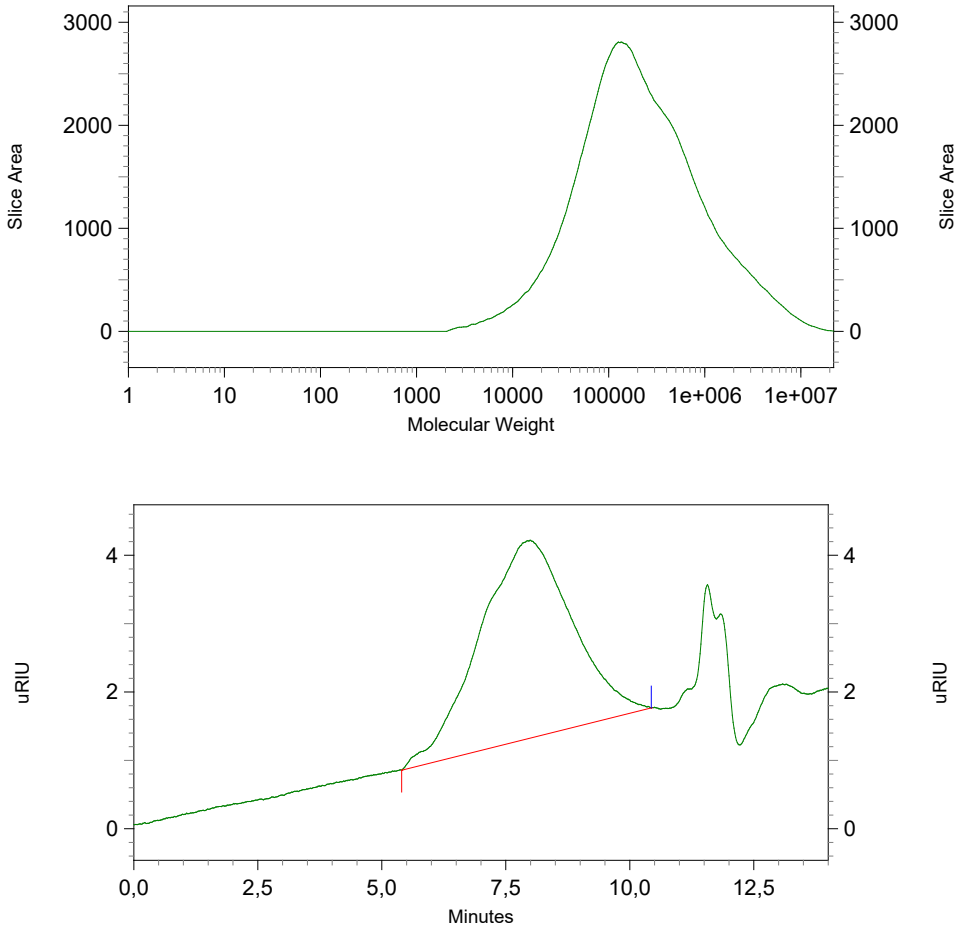

Figure S35. GPC of poly(1-hexene) (Table 2, Entry 5).

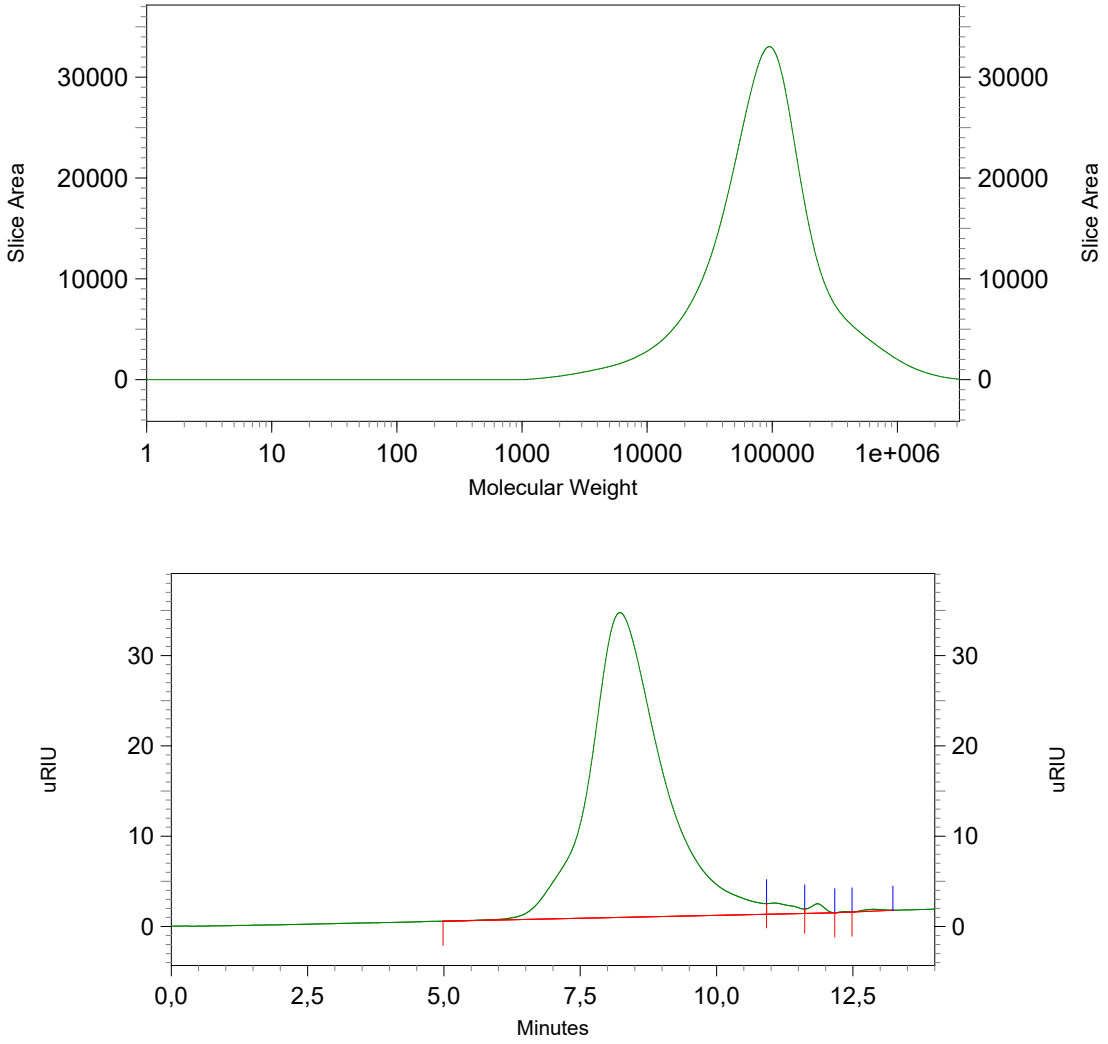

Figure S36. GPC of poly(1-hexene) (Table 2, Entry 6).

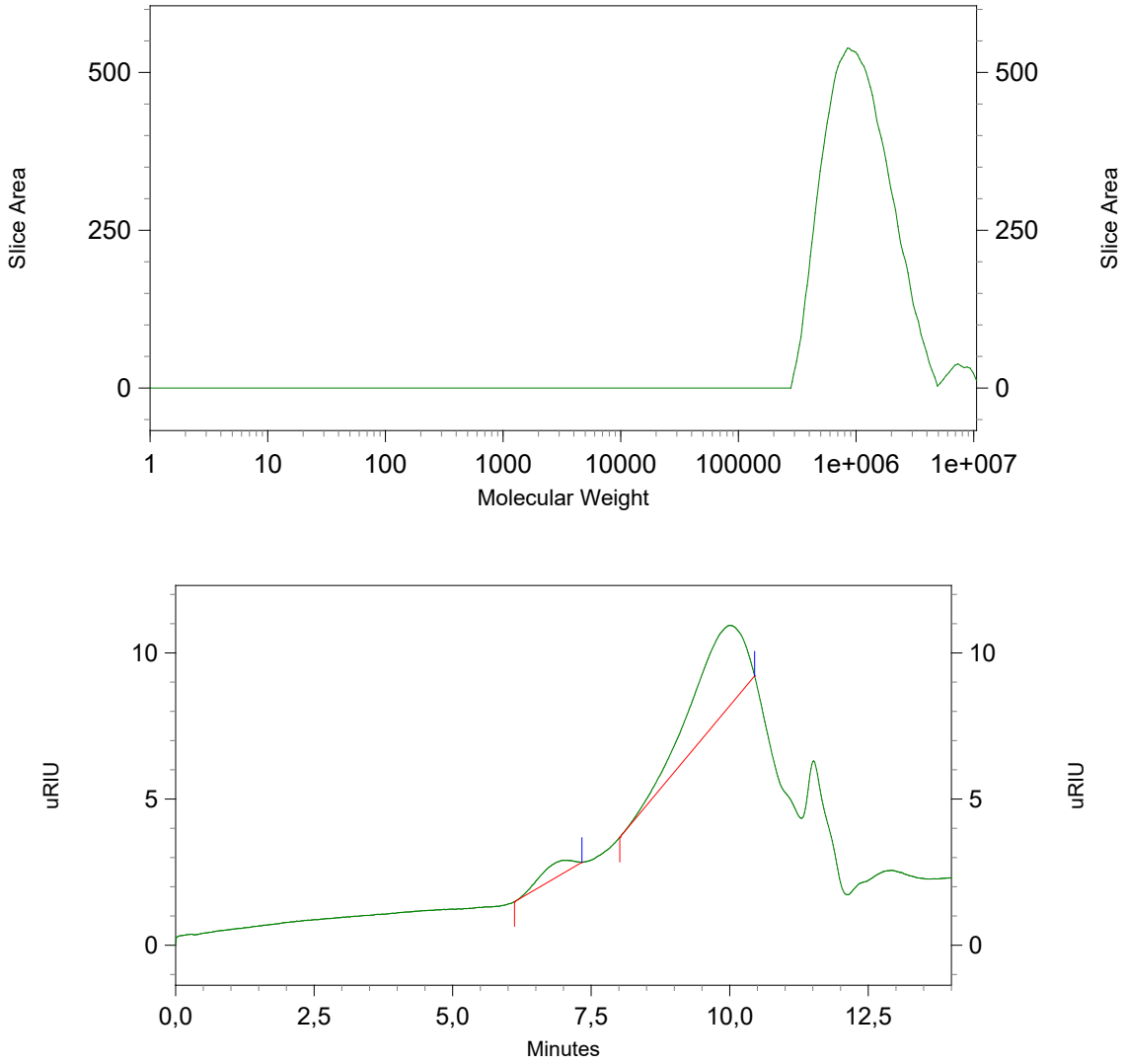

Figure S37. GPC of poly(1-hexene) (Table 2, Entry 7).

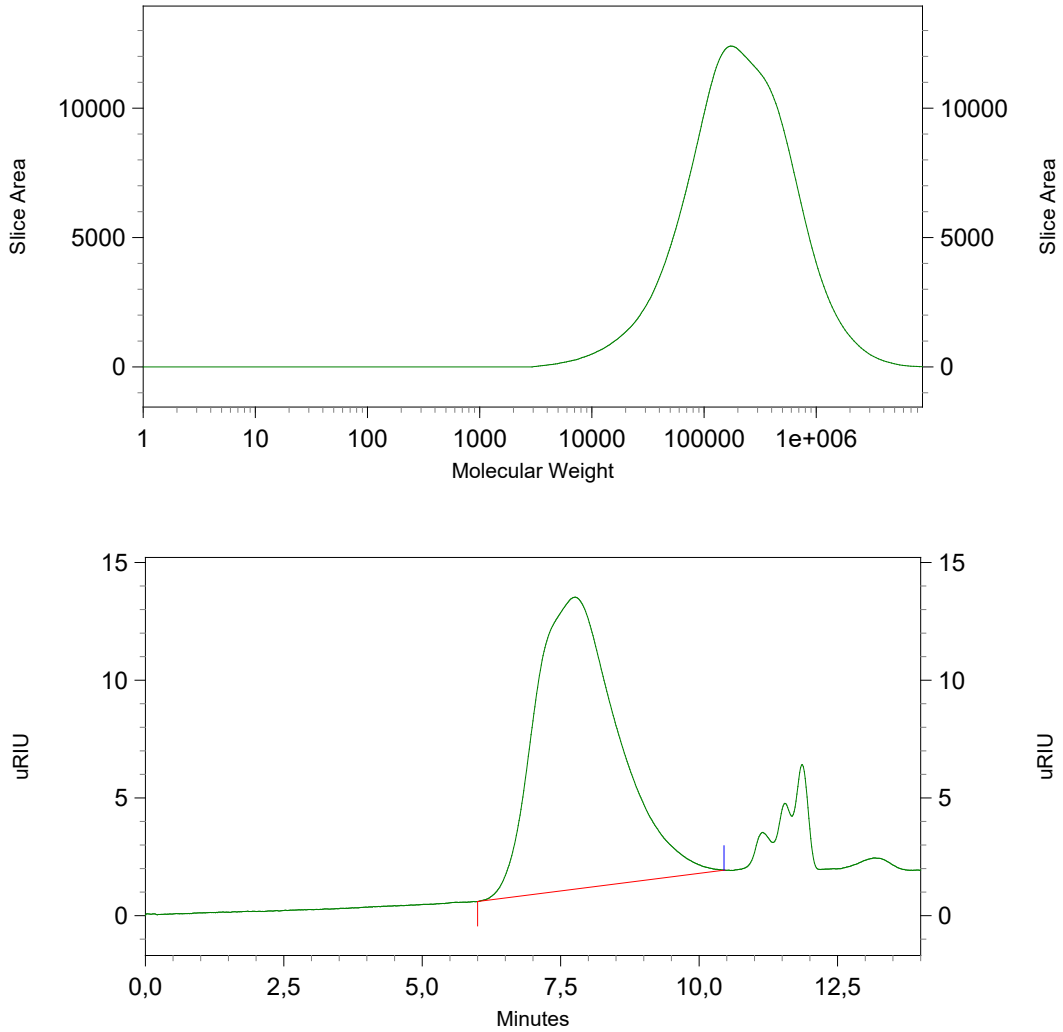

Figure S38. GPC of poly(1-hexene) (Table 2, Entry 8).

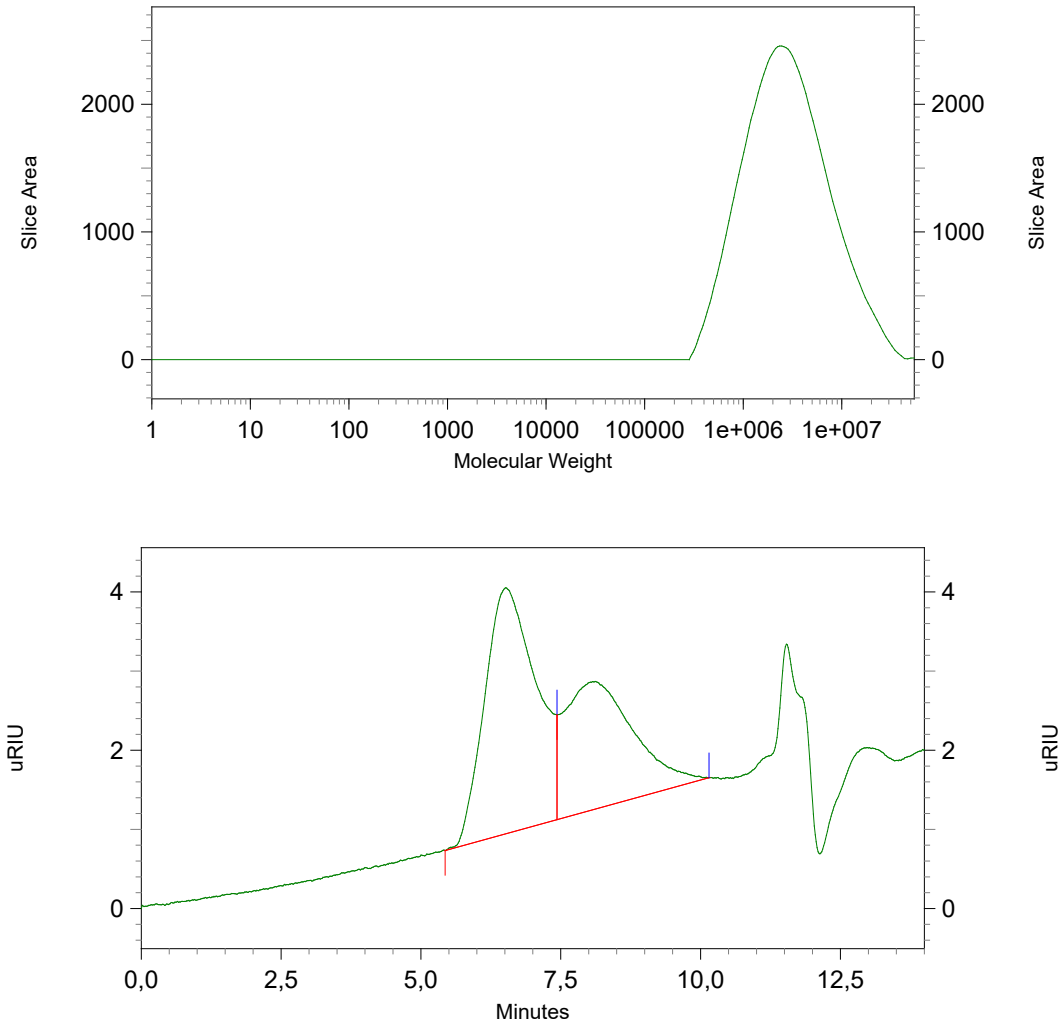

Figure S39. GPC of poly(1-hexene) (Table 2, Entry 9).

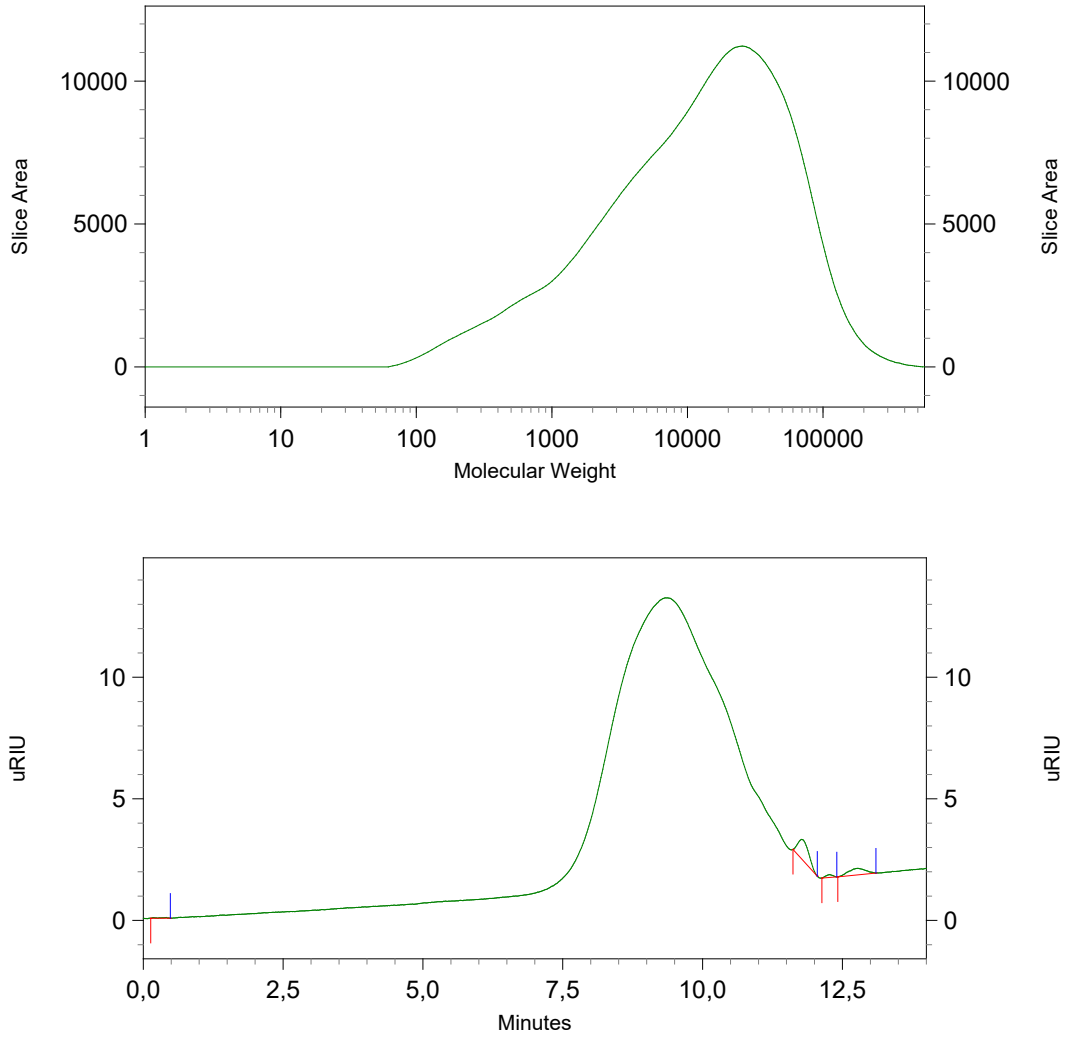

Figure S40. GPC of poly(1-hexene) (Table 2, Entry 10).

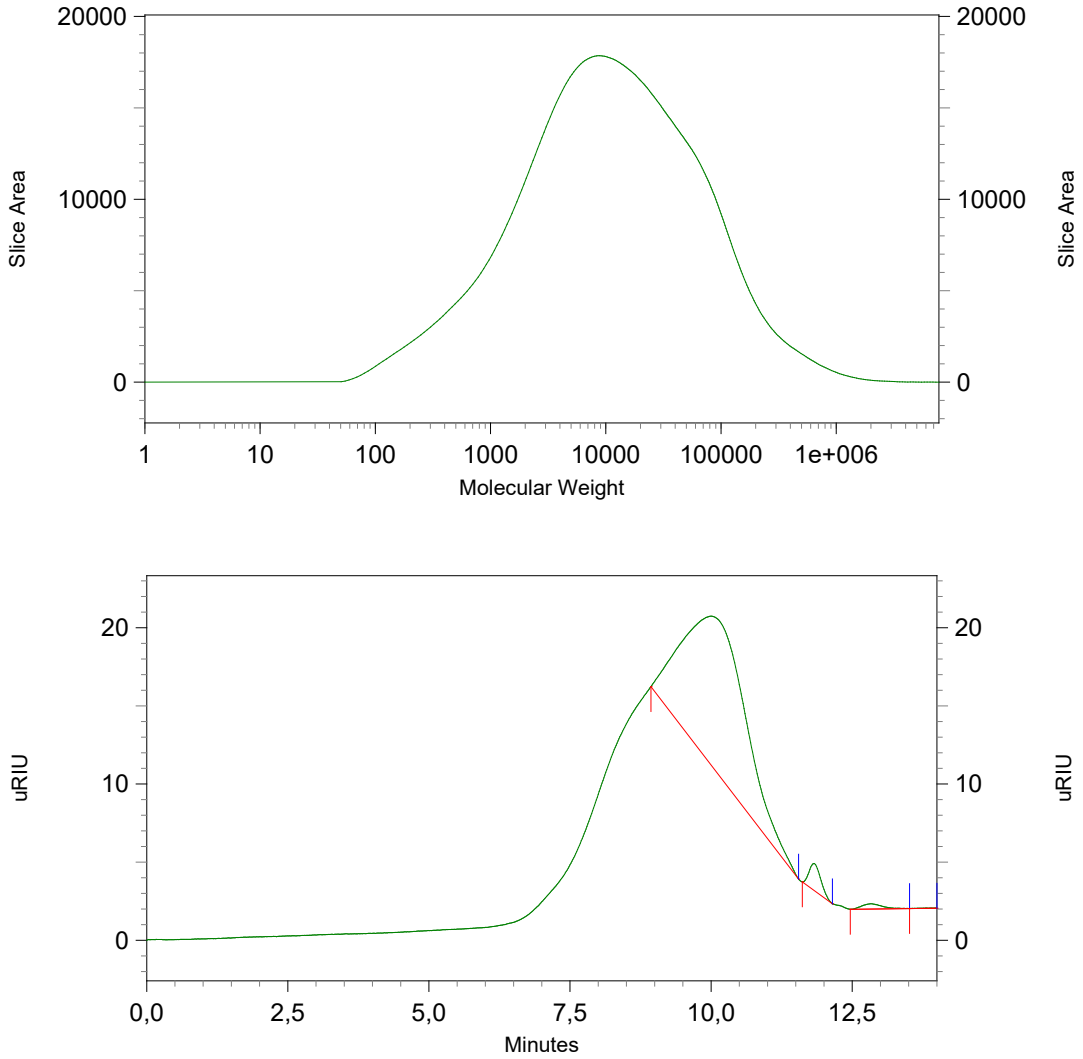

Figure S41. GPC of poly(1-hexene) (Table 2, Entry 11).

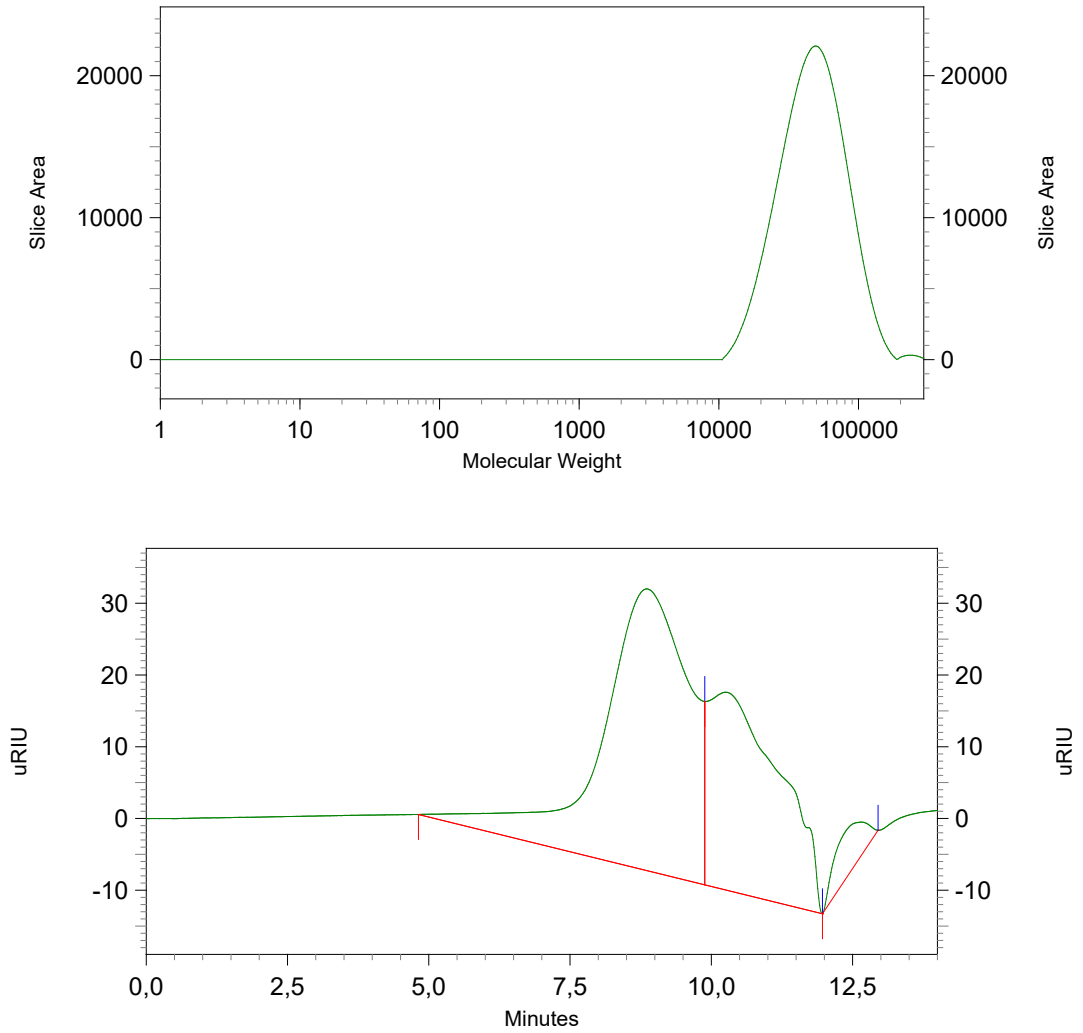

Figure S42. GPC of poly(1-heptene) (Table 2, Entry 12).

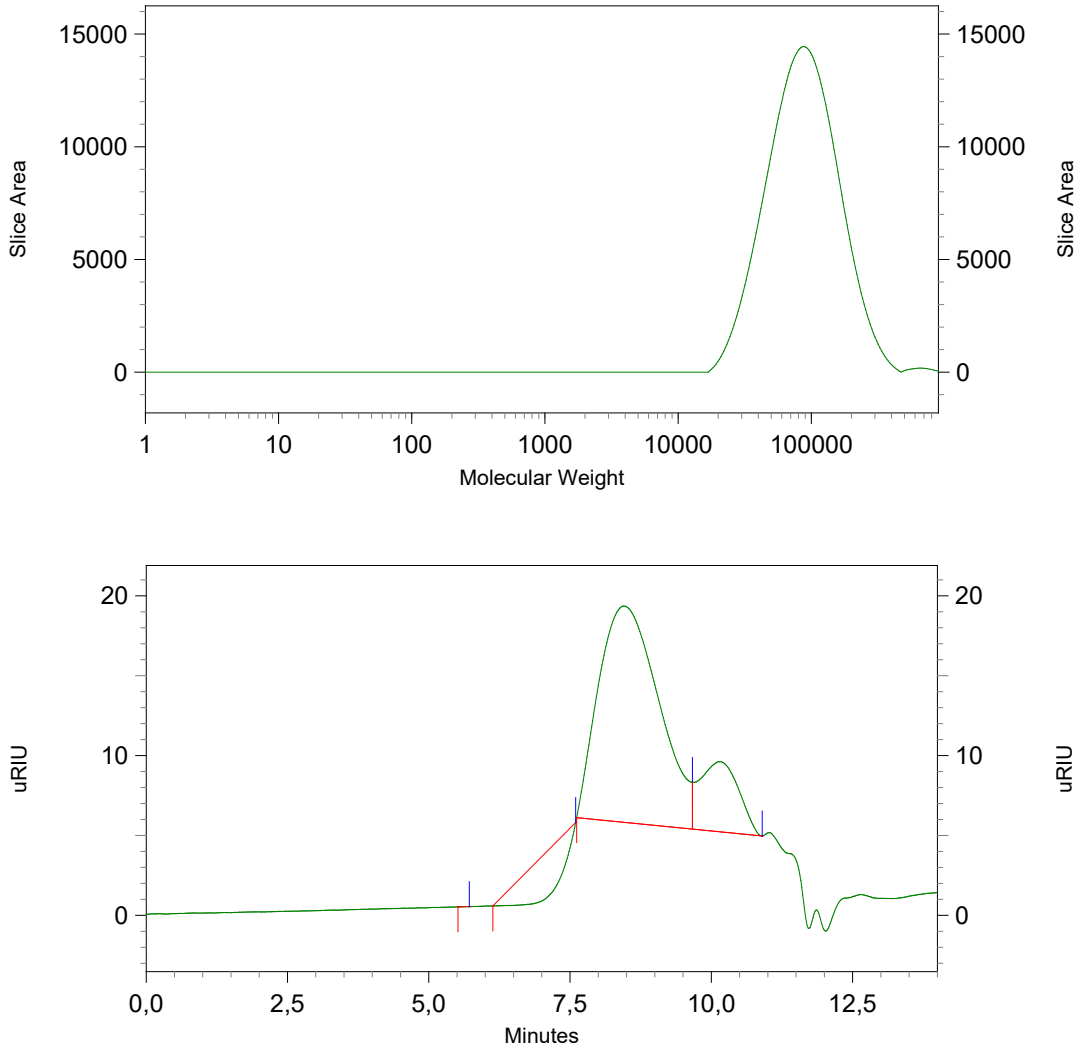

Figure S43. GPC of poly(1-octene) (Table 2, Entry 13).

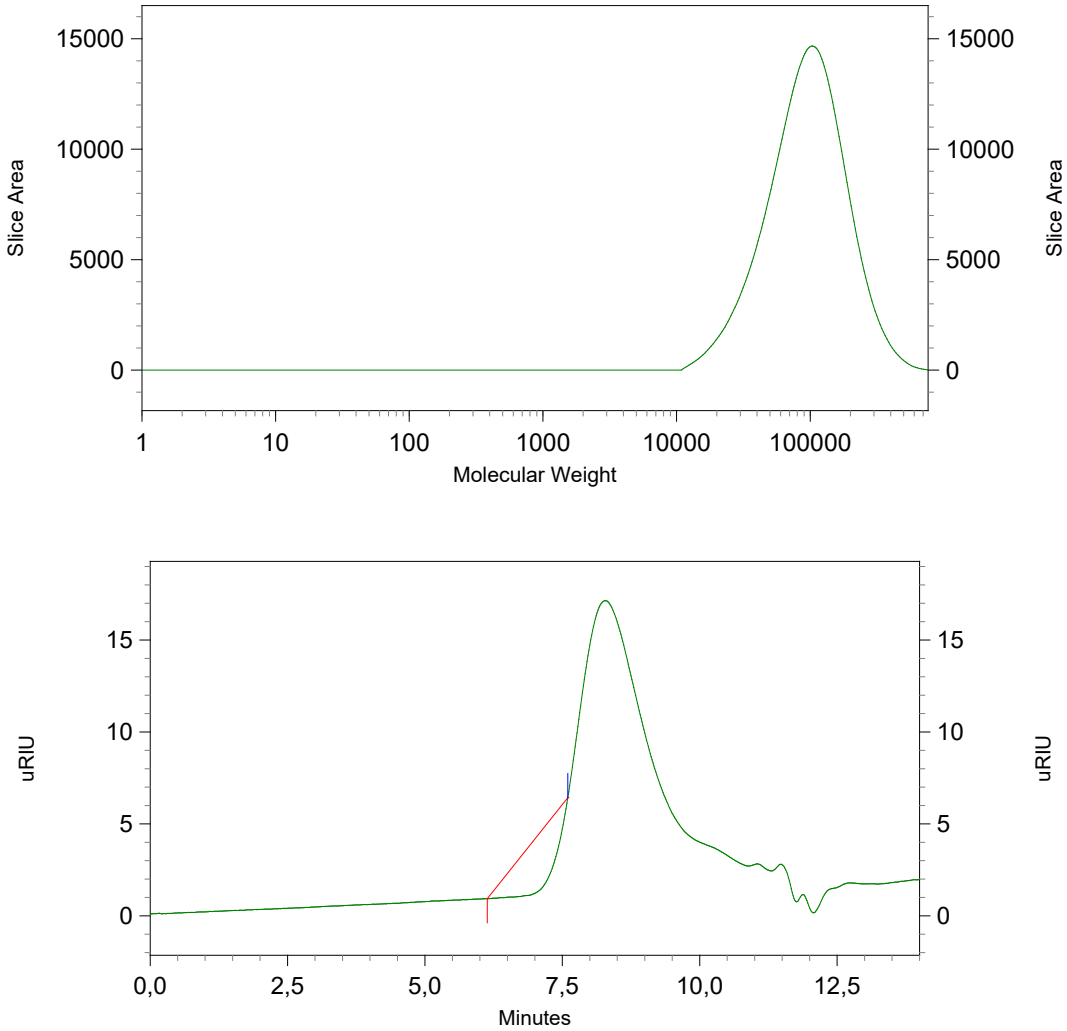

Figure S44. GPC of poly(1-nonene) (Table 2, Entry 14).

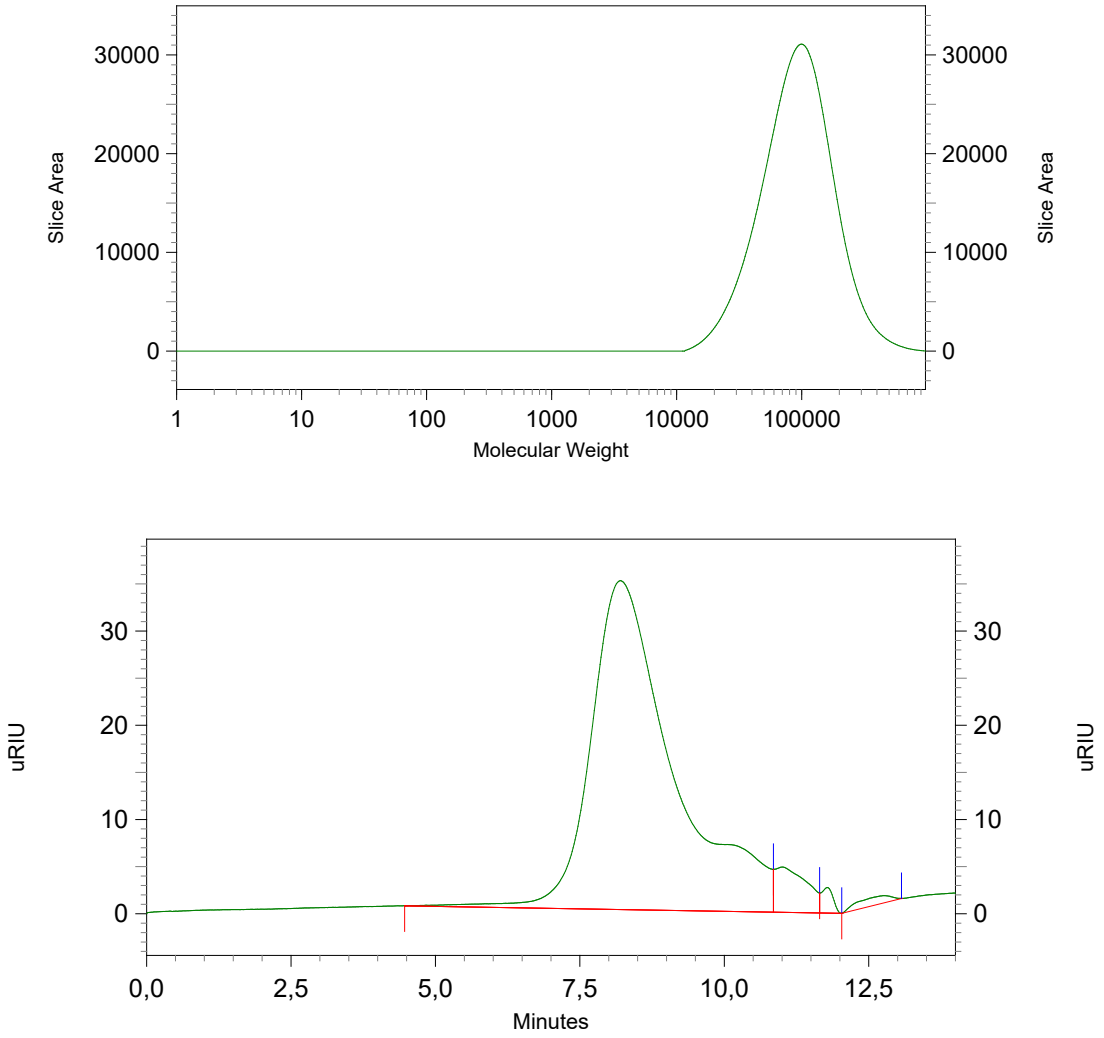

Figure S45. GPC of poly(1-decene) (Table 2, Entry 15).

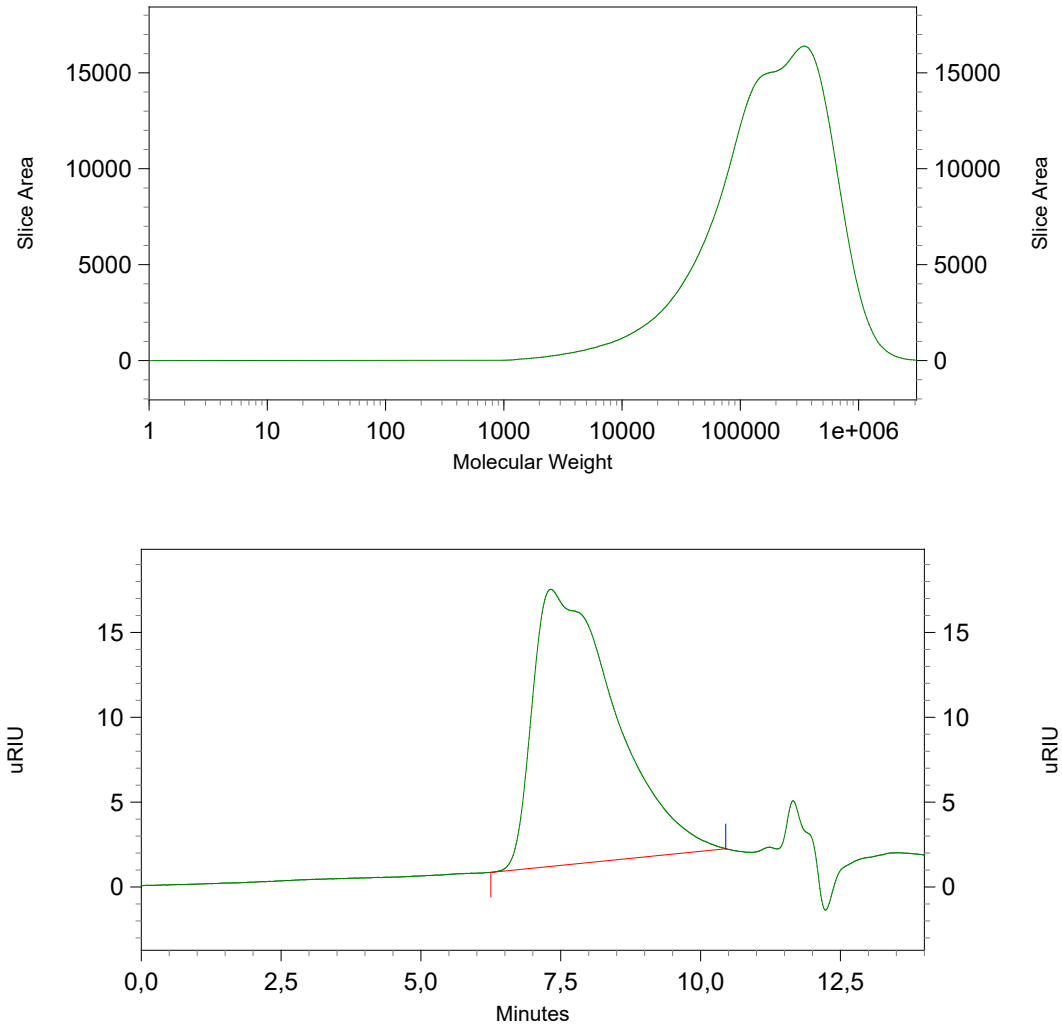

Figure S46. GPC of poly(1-decene) (Table 2, Entry 16).

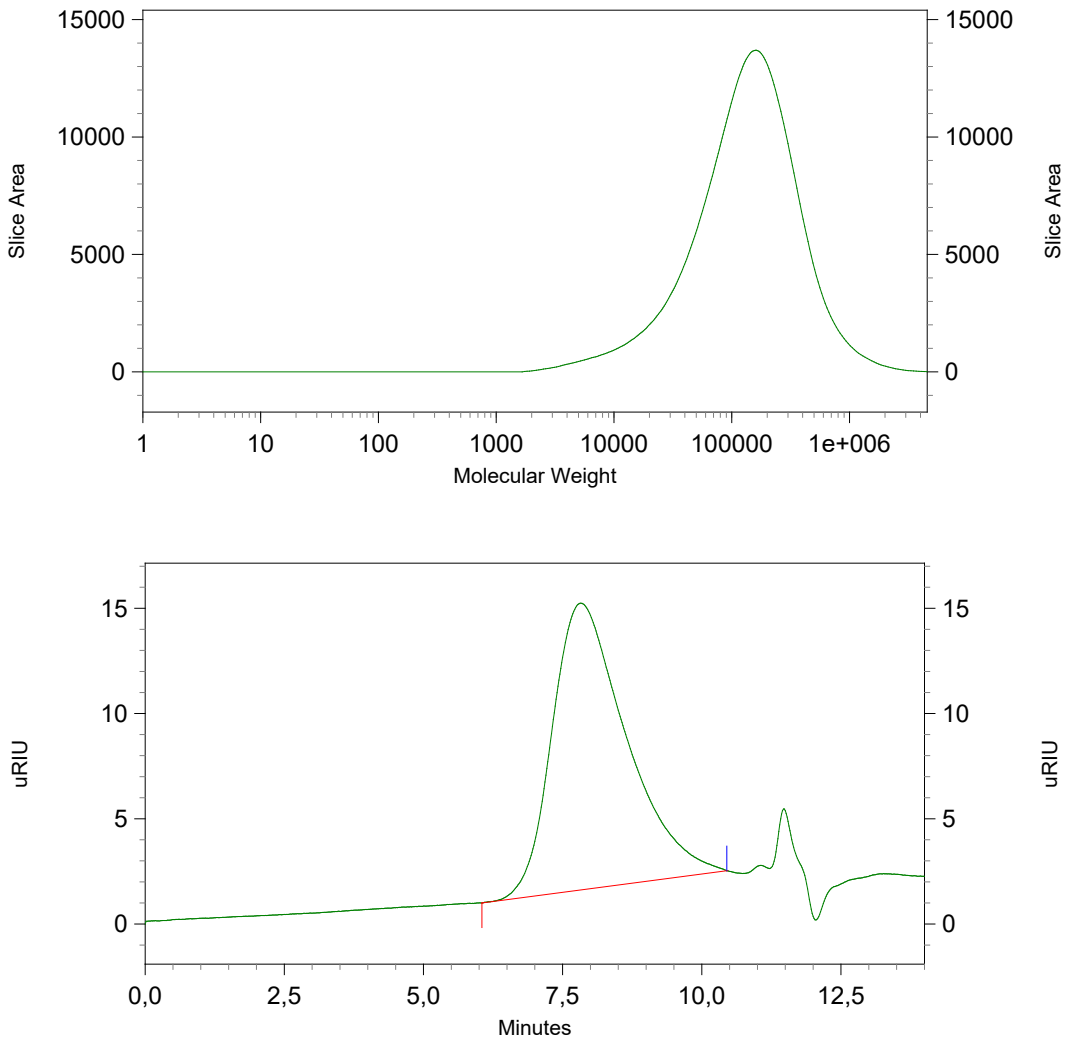

Figure S47. GPC of poly(1-decene) (Table 2, Entry 17).

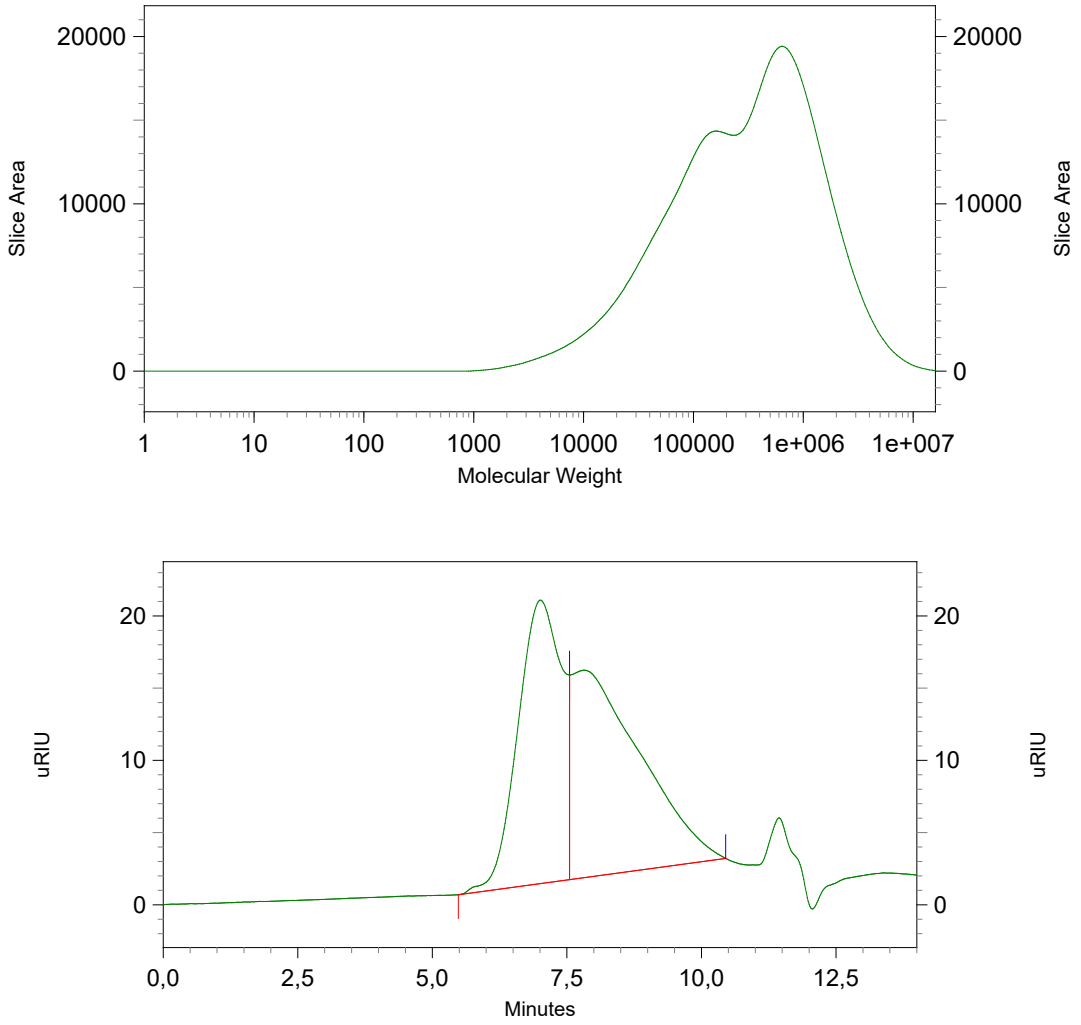

Figure S48. GPC of poly(1-decene) (Table 2, Entry 18).

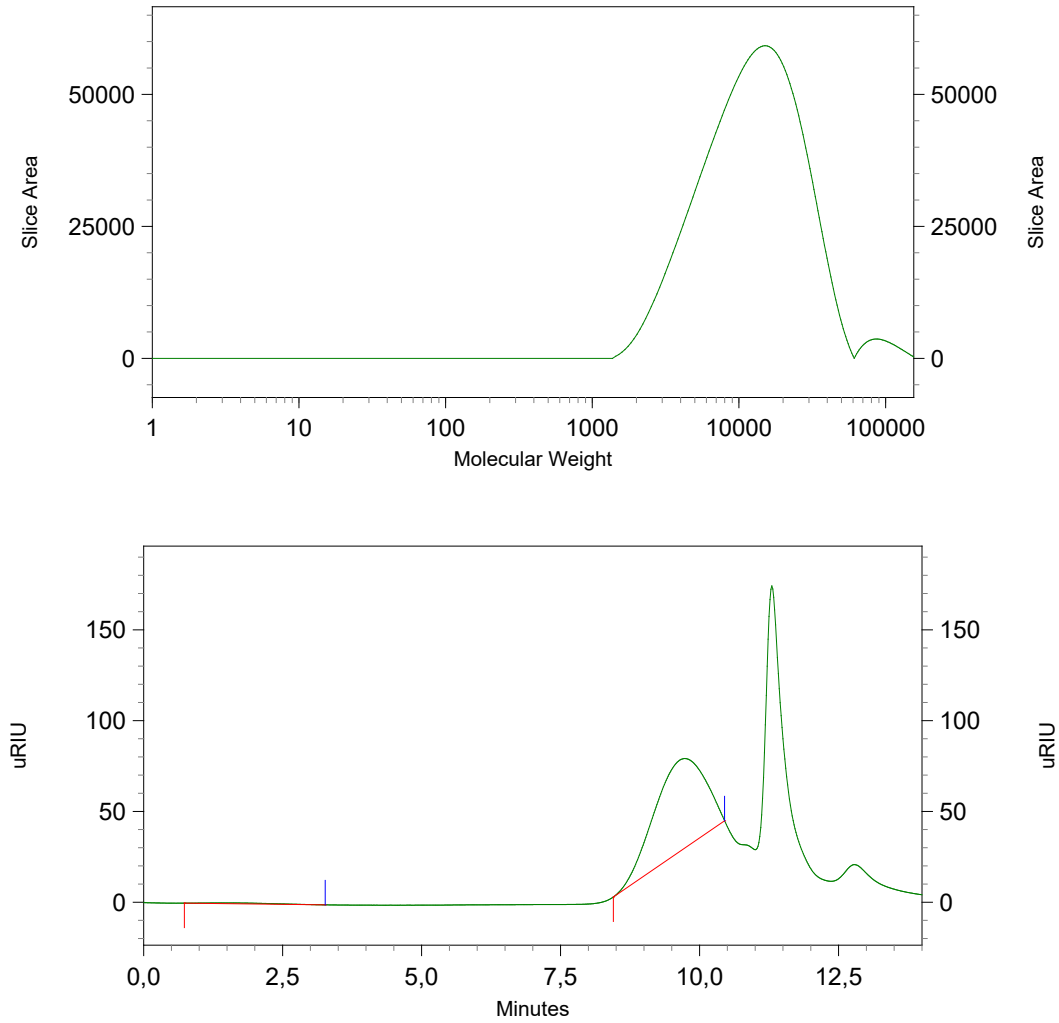

Figure S49. GPC of poly(4,4-diphenyl-but-1-ene) (Table 2, Entry 19).

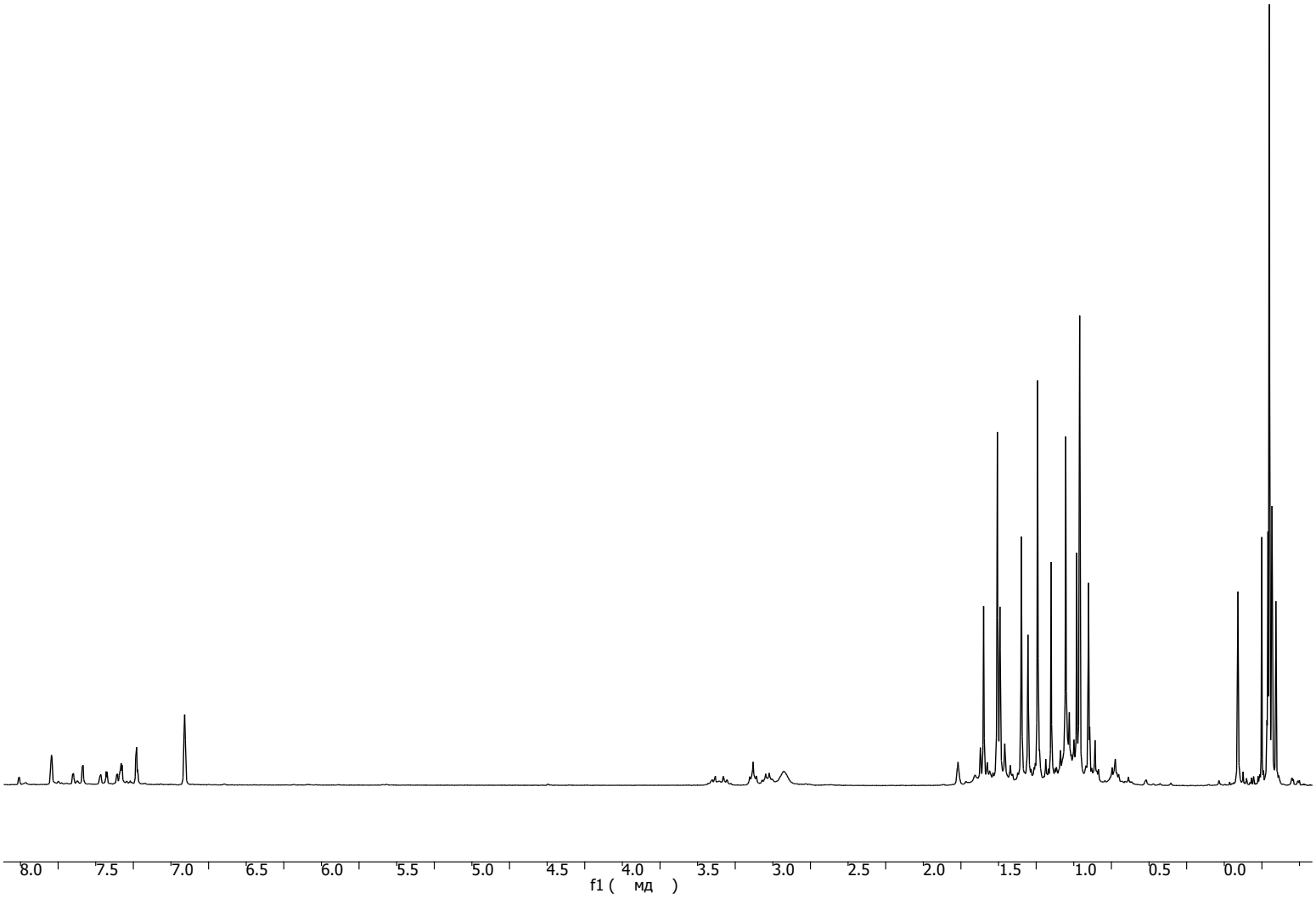

Figure S50. ^{1}H NMR spectrum of the reaction of **3-Sc** with $B(C_6F_5)_3$ (300 MHz, C_6D_6, 300 K).

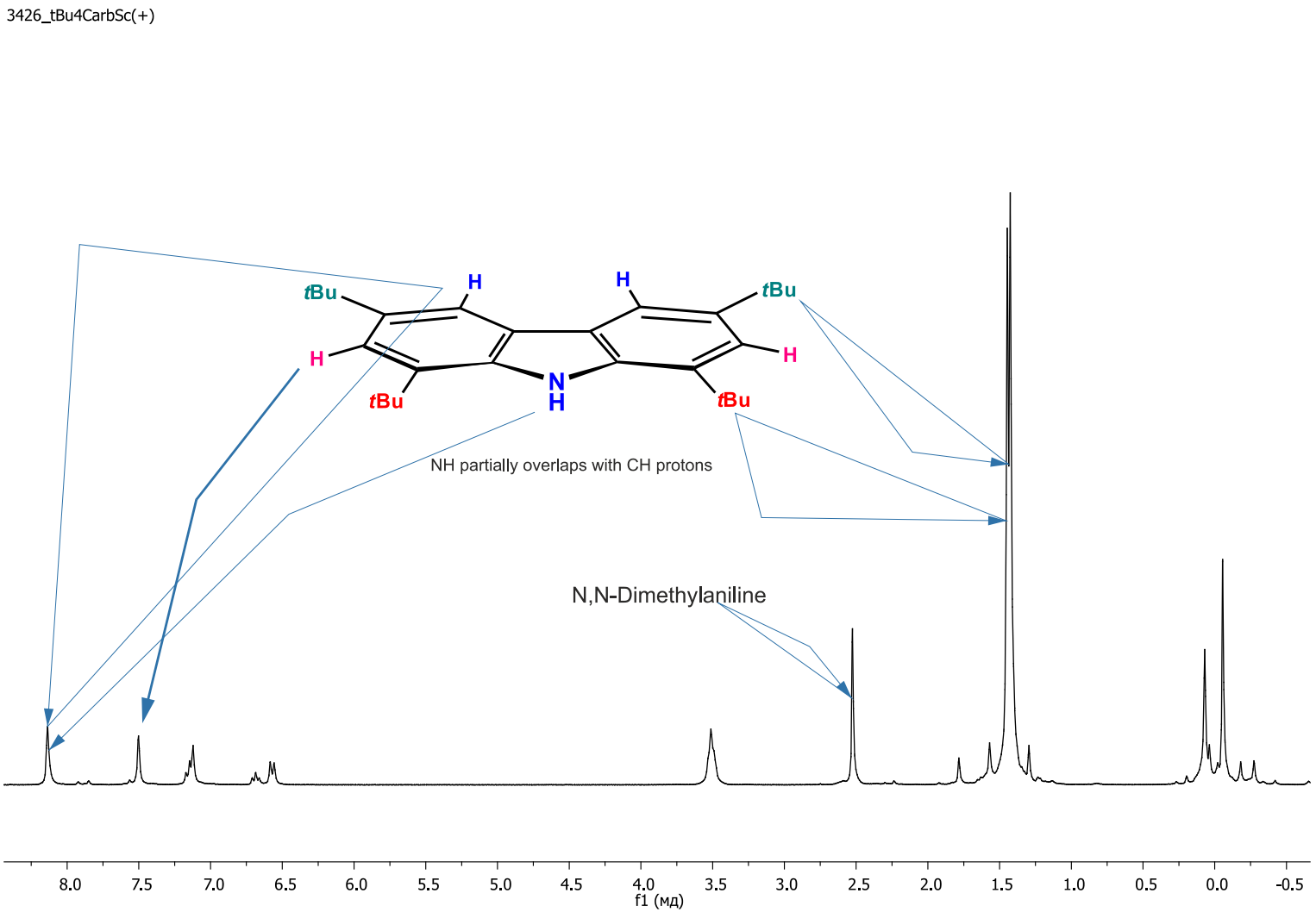

Figure S51. ^{1}H NMR spectrum of the reaction of **3-Sc** with $[PhNHMe_2][B(C_6F_5)_4]$ (300 MHz, C_6D_6, 300 K).

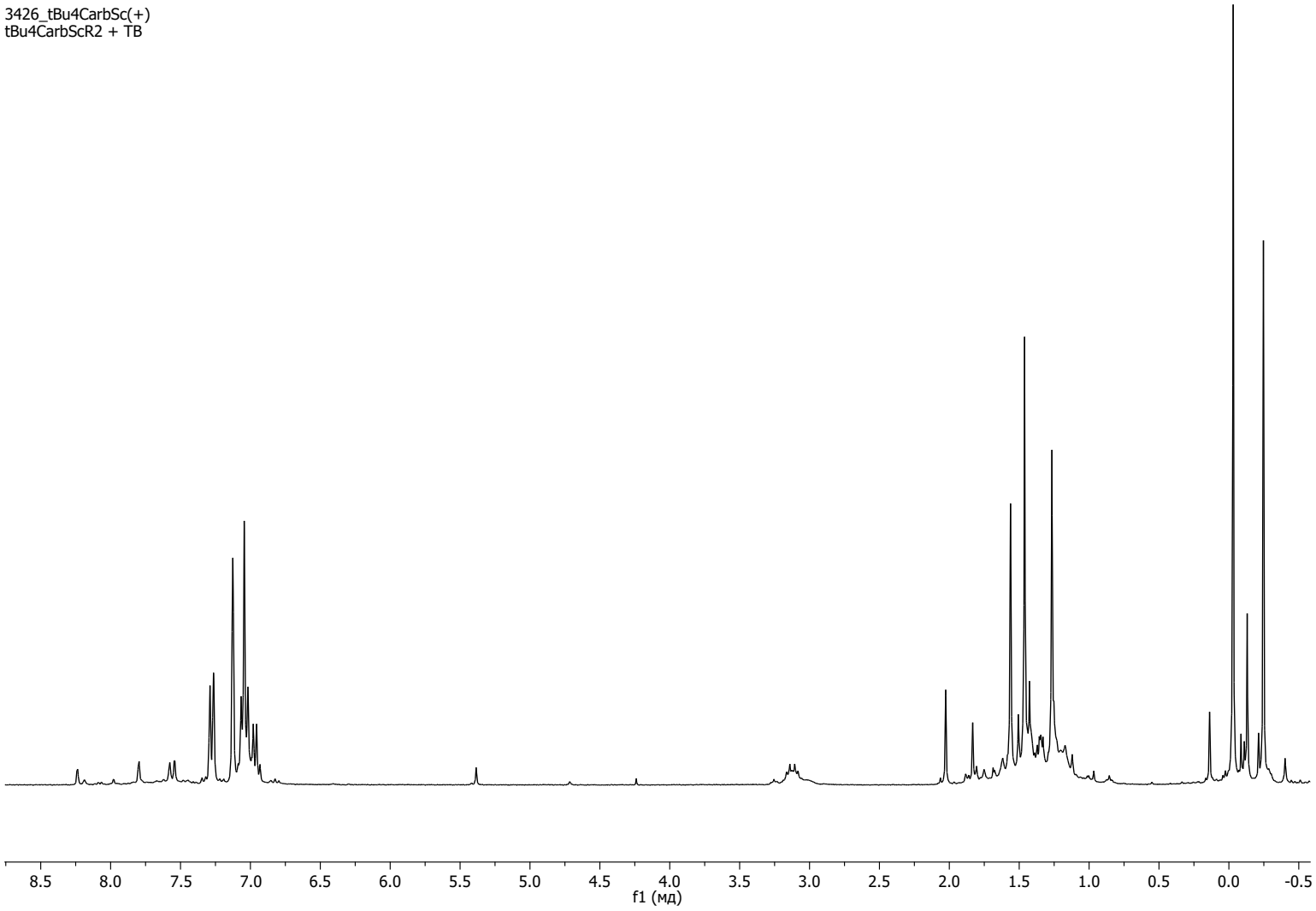

Figure S52. ^{1}H NMR spectrum of the reaction of **3-Sc** with $[Ph_3C][B(C_6F_5)_4]$ (300 MHz, C_6D_6, 300 K).

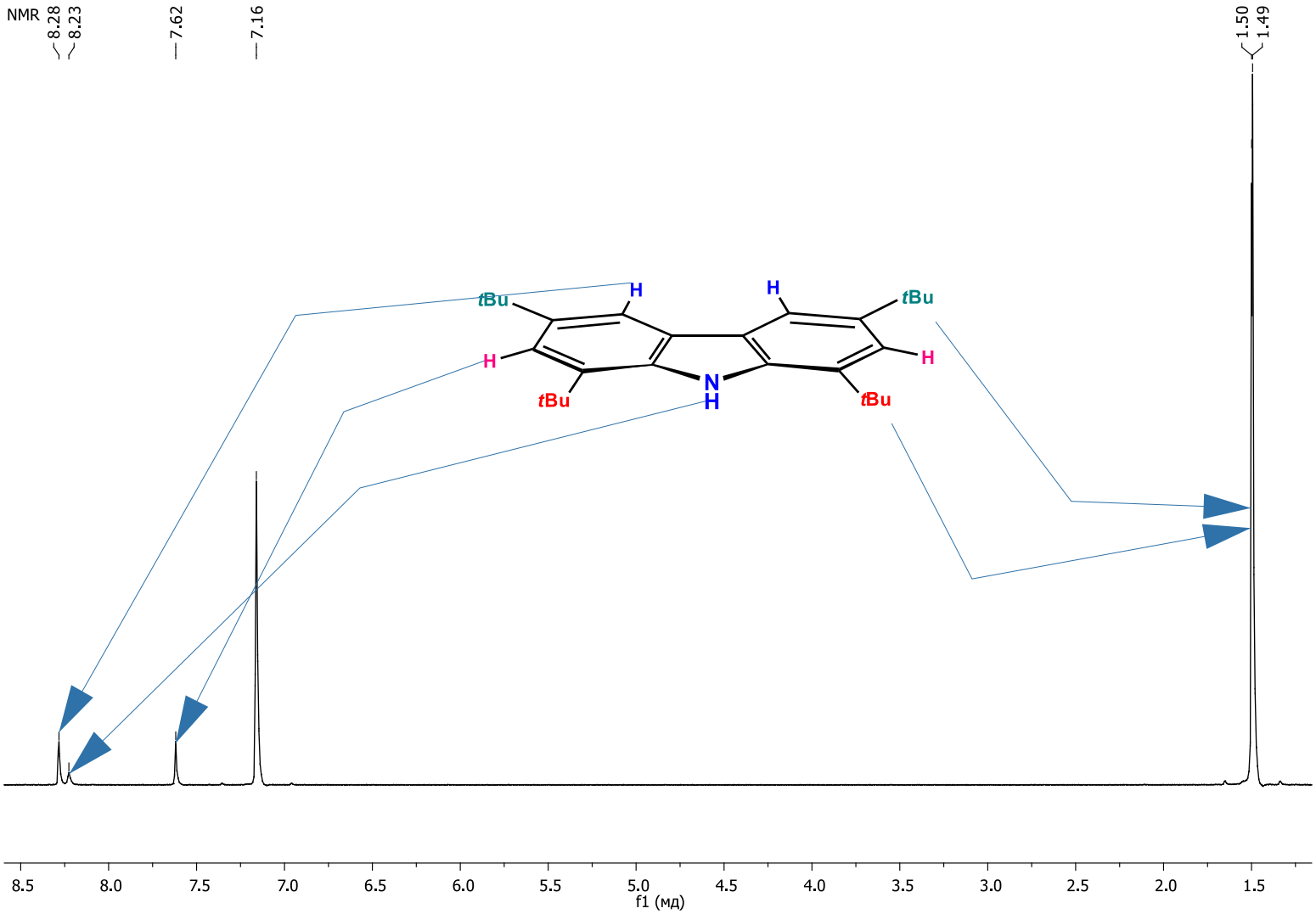

Figure S53. ^{1}H NMR spectrum of the tBu$_4$CarbH (400 MHz, C_6D_6, 298 K).

Table S1. Crystal Data and Structure Refinement Details for Complexes **1-La**, **2-Y**, **2-Sc**, **3-Sc**

	1-La	**2-Y**	**2-Sc**	**3-Sc**
Empirical formula	$C_{46}H_{62}LaNO$	$C_{46}H_{64}N_3Y$, C_7H_8	$C_{46}H_{64}N_3Sc$, ½C_6H_{14}	$C_{40}H_{70}NOScSi_2$, C_5H_{12}
Formula weight	783.87	840.04	747.04	754.25
T, K	100	120	120	100
Crystal system	Triclinic	Monoclinic	Monoclinic	Monoclinic
Space group	*P-1*	*P2₁/c*	*C2/c*	*P2₁/c*
a, Å	10.4113(3)	21.112(13)	41.78(2)	10.9924(5)
b, Å	10.6661(3)	12.629(8)	12.672(6)	15.8617(7)
c, Å	19.7627(6)	18.607(11)	18.072(8)	27.3052(12)
α, deg	88.4910(10)	90	90	90
β, deg	82.5190(10)	107.171(10)	112.604(12)	93.099(2)
γ, deg	68.7340(10)	90	90	90
V, Å^3	2027.24(10)	4740(5)	8833(7)	4753.9(4)
Z	2	4	8	4
d_{calc}, g/cm^3	1.284	1.177	1.124	1.054

μ, mm^{-1}	1.087	1.267	0.202	0.236
F_{000}	820	1800	3256	1664
Crystal size, mm	0.25×0.11×0.04	0.10×0.10×0.01	0.35×0.15×0.03	0.17×0.09×0.05
θ range for data collection, deg	2.05-27.89	1.90-26.02	1.69-25.03	2.26-25.12
HKL indices	-13≤h≤13, -14≤k≤14, -25≤l≤25	-26≤h≤26, -15≤k≤15, -22≤l≤22	-49≤h≤49, -15≤k≤15, -21≤l≤21	-13≤h≤13, -18≤k≤18, -32≤l≤32
Reflns collected	20152	60951	59336	53000
Independent reflns ($I > 2\sigma(I)$)	8292	4041	3097	5769
R_{int}	0.0246	0.4026	0.5174	0.1048
Compl. to θ, %	99.1	99.9	99.9	99.6
Data / restraints / params	9575 / 0 / 470	9335 / 699 / 572	7787 / 585 / 524	8443 / 182 / 550
$S(F^2)$	1.060	0.991	1.002	1.042
Final *R* indices ($F^2 > 2\sigma(F^2)$)	R_1 = 0.0312, wR_2 = 0.0703	R_1 = 0.0806, wR_2 = 0.1258	R_1 = 0.1175, wR_2 = 0.2627	R_1 = 0.0579, wR_2 = 0.1146
R indices (all data)	R_1 = 0.0406,	R_1 = 0.2129,	R_1 = 0.2802,	R_1 = 0.1027,

	$wR_2 = 0.0733$	$wR_2 = 0.1616$	$wR_2 = 0.3567$	$wR_2 = 0.1318$
Largest diff peak and hole, e/Å^3	1.13 / -1.01	0.55 / -0.56	1.07 / -0.74	0.41 / -0.40